Recent advances on push–pull organic dyes as visible light photoinitiators of polymerization

Corentin Pigot, Guillaume Noirbent, Damien Brunel, Frederic Dumur

Contents lists available at ScienceDirect

European Polymer Journal

journal homepage: http://ees.elsevier.com

Recent advances on push–pull organic dyes as visible light photoinitiators of polymerization

Corentin Pigot, Guillaume Noirbent, Damien Brunel, Frédéric Dumur

Aix Marseille Univ, CNRS, ICR, UMR 7273, F-13397 Marseille, France

ARTICLE INFO

Keywords
Photoinitiator
Push–pull dyes
Photopolymerization
LED
Visible light
Low light intensity
Panchromatic
Indanedione

ABSTRACT

Photoinitiators activable under visible light and low light intensity are actively researched as it can advantageously address the safety concerns raised by the traditional UV-light photopolymerization process as well as the light penetration issue. Among dyes strongly absorbing in the visible range, one of the most promising family of photoinitiators are push–pull dyes based on an electron-donating and an electron-accepting moiety connected at both ends of a polyenyl-type spacer. By acting on both the strength of the electron donor and the electron acceptor, position of the intramolecular charge transfer (ICT) band can be easily tuned from the near-UV to the near infrared region. In this review, an overview of the different D-π-A push–pull dyes used as visible photoinitiators of polymerization is presented. Over the years, a clear evolution in the chemical structure of the electron acceptors can be clearly observed, evidencing the strong activity existing around these structures.

1. Introduction

During the last decades, photoinitiators activable under visible light and low light intensity have focused intensive research efforts due to the wide range of applications requiring these structures [1]. If photopolymerization was traditionally devoted to the polymerization of coatings and adhesives due to the wavelength used during the pioneering works in photopolymerization (i.e. UV-light), [2-4] the scope of applications has recently been extended to emerging fields such as micro and nanoelectronics, 3D and 4D-printing [5-11]. Photopolymerization exhibits several appealing features compared to the traditional solution phase polymerization. Notably, a spatial and temporal control can be obtained [12,13]. Photopolymerization consists in converting a liquid resin into a solid material and this chemical transformation can be carried out in solvent-free conditions, avoiding the release of volatile organic compounds [14-16]. As other advantages, the polymerization process can also be extremely fast and no workup is required subsequent to the polymerization process and the reaction can be done in solvent-free conditions (See Fig. 1). As the driving force for initiating the polymerization reaction, light typically act as a traceless reagent with which no side product remains after polymerization. Recently, photopolymerization under visible light has attracted a great deal of efforts by the improved light penetration of the visible light compared to the UV light. Thus, if light penetration is limited to a few hundreds of micrometers at 300 nm, this latter can be increased until 5 cm at 800 nm, revolutionizing the scope of applications of photopolymerization [17].

Concomitant to the development of visible light photoinitiating systems, cheap, compact and lightweight irradiation setups have been developed such as the Light-emitting Diodes (LEDs) or the Laser diodes making the traditional irradiation systems obsolete. Over the years and in order their absorption spectra to perfectly fit with the emission spectra of the different visible light sources, a wide range of structures have been examined as visible light photoinitiators such as acridones **1**, [18,19] acridine-1,8-dione **2**, [20,21] benzophenones **3**, [22-25] camphorquinones **4**, [26,27] carbazoles **5**, [28-33] chalcones **6**, [34,35] chromones **7**, [36-38] coumarins **8**, [39-43] copper complexes **9**, [44-54] cyclohexanones **10**, [55-57] dihydroanthraquinone **11**, [58] 2,3-diphenylquinoxaline derivatives **12**, [59] diketopyrrolopyrrole **13**, [60-62] flavones **14**, [63,64] ferrocenes **15**, [65,66] helicenes **16**, [67,68] iodonium salts **17**, [66,69,70] iridium complexes **18**, [71-76] iron complexes **19**, [77-81] naphthalimides **20**, [82-93] perylenes **21**, [94-96] phenothiazines **22**, [97] porphyrins **23**, [98,99] pyrenes **24**, [100-105] squaraines **25**, [98] thioxanthones **26** [106-109] have been identified as promising scaffolds for the design of visible light photoinitiators (See Fig. 2). However, for numerous abovementioned families, the tunability of their absorption spectra remains limited. Notably, coumarins strongly absorb in the near-UV visible range [110-112] whereas perylenes [113,114] or phthalocyanines [115-118] mostly absorb beyond 550–600 nm. For most of these families, tunability of their absorption spectra remains limited

E-mail addresses: corentin.pigot@univ-amu.fr (C. Pigot); frederic.dumur@univ-amu.fr (F. Dumur)

https://doi.org/10.1016/j.eurpolymj.2020.109797
Received 30 April 2020; Received in revised form 19 May 2020; Accepted 22 May 2020
Available online xxx
0014-3057/

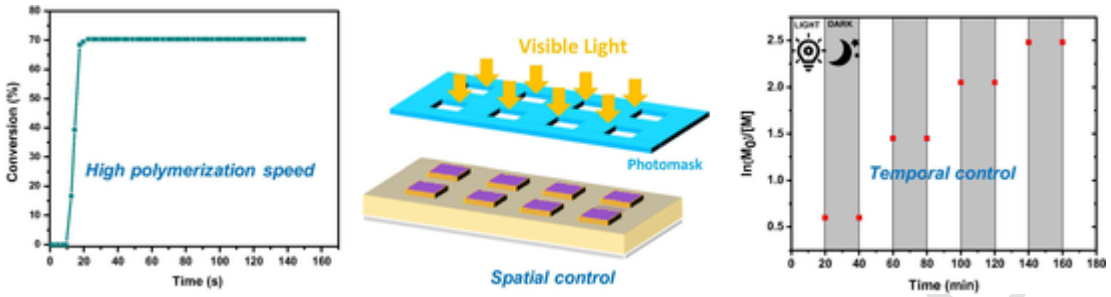

Fig. 1. Characteristics of the photopolymerization process.

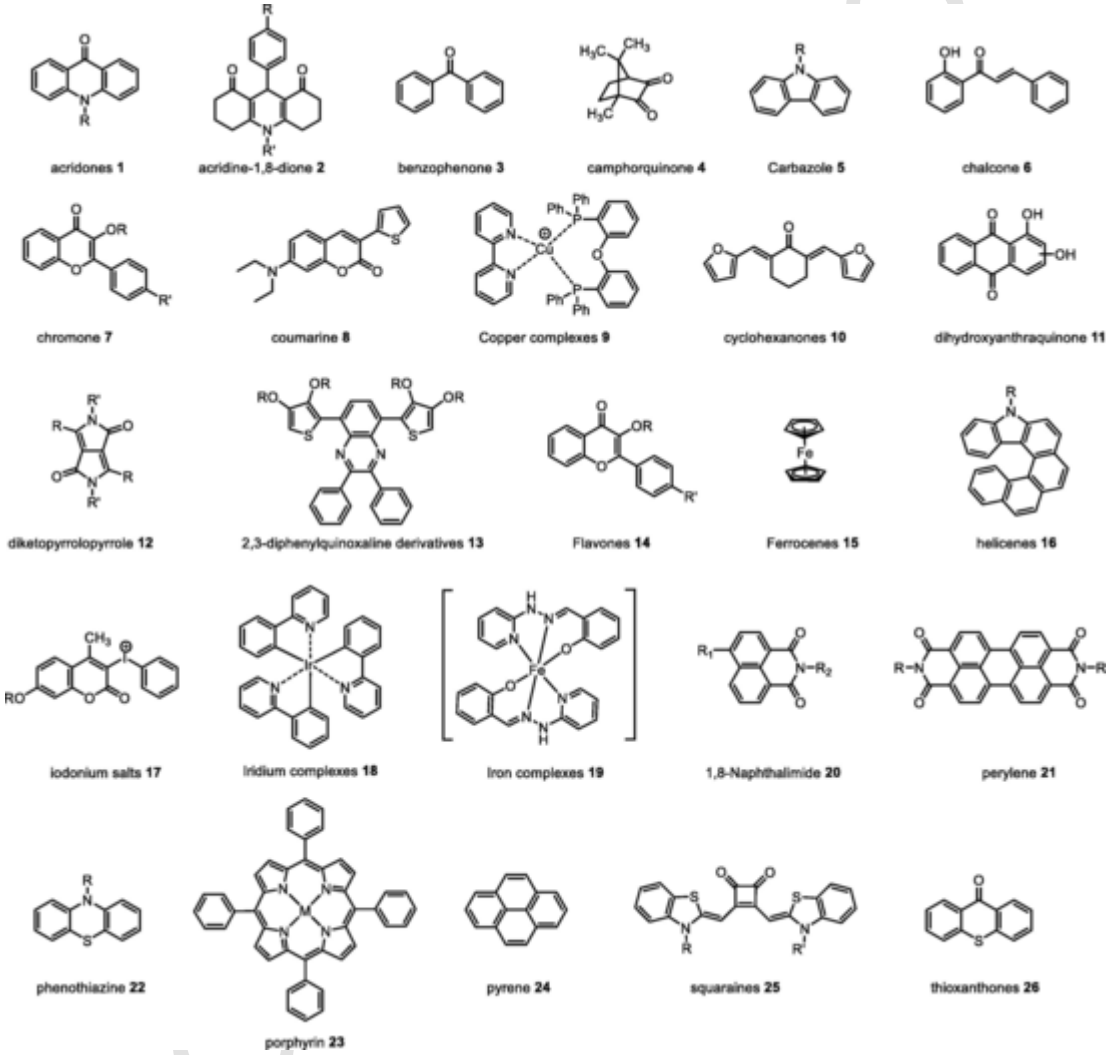

Fig. 2. Chemical structures of common visible light photoinitiators.

(coumarins, perylene, phthalocyanines) so that a red-shift or a blue-shift of their absorptions can only be obtained after extensive synthetic works. In this context, this approach is not viable from an industrial point of view.

With aim at developing photoinitiators with absorptions that can be efficiently tuned in the 400–800 nm range, push–pull dyes comprising a donor connected to an acceptor by mean of a conjugated spacer is the most straightforward route [119,120]. Indeed, absorption spectrum of D-π-A structures (where D and A respectively stand for donor and acceptor and π corresponds to the polyenic spacer) can be easily tuned by modifying the electron-donating ability of the donor or the electron-releasing ability of the acceptor. Parallel to this, elongation of the polyenic spacer enables both to redshift the absorption spectrum of the dyes by destabilizing the highest occupied molecular orbital (HOMO) without significantly affecting the position of the lowest unoccupied molecular orbital (LUMO) [121-124].

If plethora of structures exist concerning electron donors, the availability of electron accepting groups remains more limited and a few examples of the most widely used electron acceptors **A1-A18** for the design of push–pull dyes is presented in the Fig. 3. Notably, malononitrile **A1**, [125] indanedione derivatives **A2**, [126,127] (thio)barbituric derivatives **A3**, [128] Meldrum derivatives **A4**, [129] pyridinium

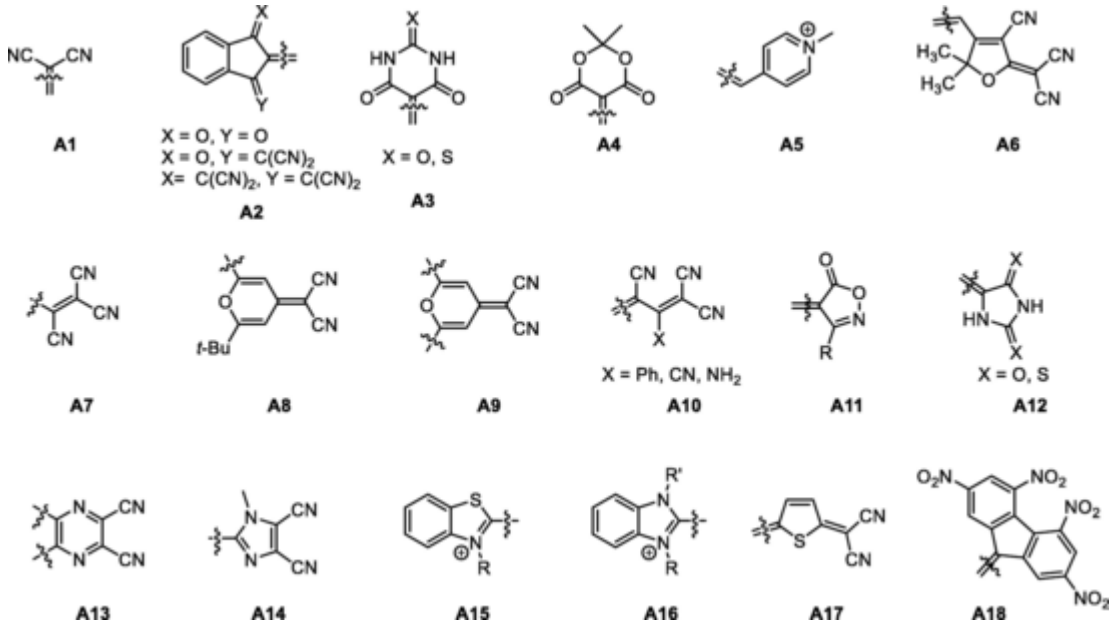

Fig. 3. Chemical structures of electron acceptors **A1-A18** commonly used for the design of push–pull dyes.

A5, [130] methyl-containing tricyanofurans **A6**, [131] substituted tricyanopropenes **A7**, [132] pyran derivatives **A8** and **A9**, [133,134] 1,1,3-tricyano-2-substituted propenes **A10**, [135] isoxazolones **A11**, [136] hydantions and rhodanines **A12**, [137] pyrazines **A13**, [138] dicyanoimidazoles **A14**, [139] benzo[*d*]thiazoliums **A15**, [140] benzo[*d*]imidazoliums **A16**, [141] dicyanovinyl-thiophen-5-ylidenes **A17** [142] and 9-methylene-2,4,5,7-tetranitro-9*H*-fluorene **A18** [143] can be mentioned. Another appealing feature of push–pull dyes is the possibility to design these structures by using a convergent approach. Indeed, the polyenyl spacer is formed in last steps by mean of a high-yielding reaction, namely the Knoevenagel reaction [144]. This reaction which was first developed by Knoevenagel in 1896 can be carried out in non-toxic solvents (often ethanol) while using a few drops of piperidine or diisopropylethylamine as the catalysts. Additionally, the reaction product can often be isolated as a solid after reaction, avoiding the use of extensive purification processes. The Knoevenagel condensation also consists in a dehydrative coupling between an aldehyde and an activated methylene group, releasing a water molecule which is a nontoxic, safe, and environmental benign side product.

Therefore, with aim at developing a wide range of structures, for a given electron-acceptor, the electron-donating groups can be easily changed, enabling to rapidly prepare numerous derivatives. The opposite situation is also true, while keeping the electron-donor constant and by varying the electron acceptors (See Scheme 1). From an application viewpoint, push pull dyes have been extensively studied for Non-linear optical applications due to their remarkable molar extinction coefficient, but also as light-absorbing materials for organic solar cells (OSCs) or as photoluminescent materials for the design of organic light-emitting diodes (OLEDs) [145-148]. In light of these different applications, especially in Organic Electronics where the ability to easily oxidize or reduce is a prerequisite, push–pull dyes have then been identified as potential candidates for photopolymerization applications. Indeed, for future development of photoinitiators, Organic Electronics is considered by photopolymerists as an El Dorado for finding innovative structures for photoinitiators [149]. Scheme 2.

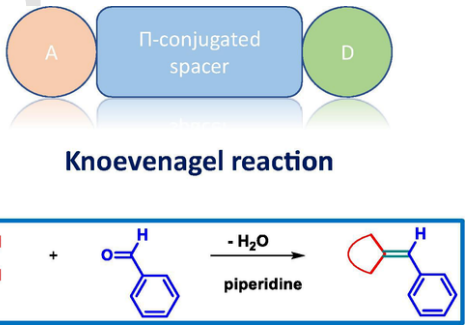

Scheme 1. Knoevenagel reaction.

In this review, an overview of the push–pull dyes used as photoinitiators of polymerization under visible light and low light intensity is presented. Considering that the push–pull effect can be obtained using numerous strategies, this review will focus on D-π-A structures comprising as electron acceptors those listed in the Fig. 2. Parallel to the synthetic route, their ability to initiate the free radical polymerization (FRP) of acrylates or the cationic polymerization (CP) of epoxides will be discussed.

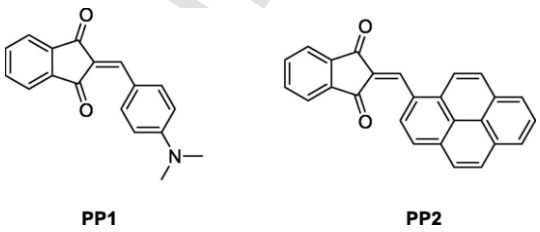

Fig. 4. Chemical structures of **PP1** and **PP2**.

2. Push-pull dyes as visible light photoinitiators of polymerization

2.1. Indane-1,3-dione derivatives

The first report mentioning the use of indane-1,3-dione-based push–pull dyes as photoinitiators was published in 2013 [150]. In this work, two structures were examined, namely **PP1** and **PP2 (See Fig. 4)**. The two dyes showed an ICT band extending from 400 to 550 nm so that polymerization tests could be carried out at 405, 457, 473 and 532 nm. Especially, molar extinction coefficients of 38 000 and 21 000 M^{-1} cm^{-1} for **PP1** and **PP2** could be determined at the maximum absorption of 478 and 464 nm, respectively.

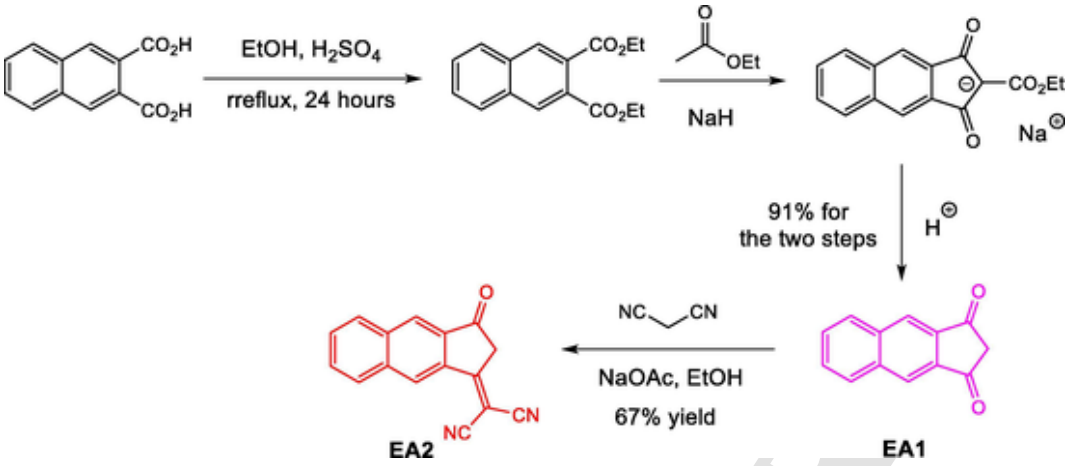

Scheme 2. Synthetic procedure of **EA1** or **EA2**.

Push-pull dyes are also characterized by their high sensitivity to their environment, and notably, the polarity/polarizability of the solvents so that position of the ICT band can drastically change from the apolar pentane to the high polar DMF or DMSO [125,130,151]. To support the experimental solvatochromism, several empirical solvent polarity scales have been developed, such as Dimroth – Reichardt's, [152] Kamlet – Taft's, [153] Catalan's, [154] Lippert – Mataga's, [155] Bakhshiev's, [156] Kawski – Chamma – Viallet's, [157] McRae's, [158] and Suppan's scales [159]. Especially, variation of the Stoke shift with the solvent polarity was examined. Interestingly, if linear correlations could be easily established for **PP2** using the Bakhshiev's, Kawski – Chamma – Viallet's, Lippert – Mataga, McRae's and Suppan's polarity scales, no reasonable linear correlations could be found for **PP1** irrespective of the polarity scale (See Fig. 5). The less linear solvatochromic behavior of **PP1** was assigned to the strong electron-donating ability of the 4-dimethylaminobenzene moiety, but also to the possibility for this group, to initiate hydrogen bonds with the solvent molecules, impacting its solvatochromism. In the two cases, the negative slopes are indicative a major charge redistribution upon photoexcitation, resulting in a significant change of the dipole moment

[160-162]. While examining the CP of (3,4-epoxycyclohexane)methyl 3,4-epoxycyclohexylcarboxylate (EPOX) for the two component **PPx**/Iod system (0.3%/2% w/w) (where Iod stands for diphenyliodonium hexafluorophosphate) upon irradiation with a Laser Diode at 473 nm (100 mW/cm^2), a fast polymerization process could be detected with **PP1** whereas no polymerization could be initiated with **PP2**. This unexpected behavior was confirmed with the more reactive three-component photoinitiating system **PPx**/NVK/Iod (0.3%/3%/2% w/w) for which no polymerization could be still detected. While irradiating at different wavelengths, variation of the final monomer conversions from 40% at 405 and 532 nm to 80% at 473 nm can be assigned to the modifications of the molar extinction coefficients at the different irradiation wavelengths (See Fig. 6).

Examination of the CP of a second monomer i.e. triethylene glycol divinyl ether DVE-3 confirmed the remarkable photoinitiating ability of **PP1**, with a monomer conversion of 95% after only 30 s. **PP1** proved also to efficiently initiate the FRP of trimethylolpropane triacrylate (TMPTA) (see Fig. 7), a monomer conversion of 50% being obtained within 200 s for the three-component system **PP1**/NVK/Iod (0.3%/3%/2% w/w) upon irradiation at 473 nm in laminate. However, no FRP

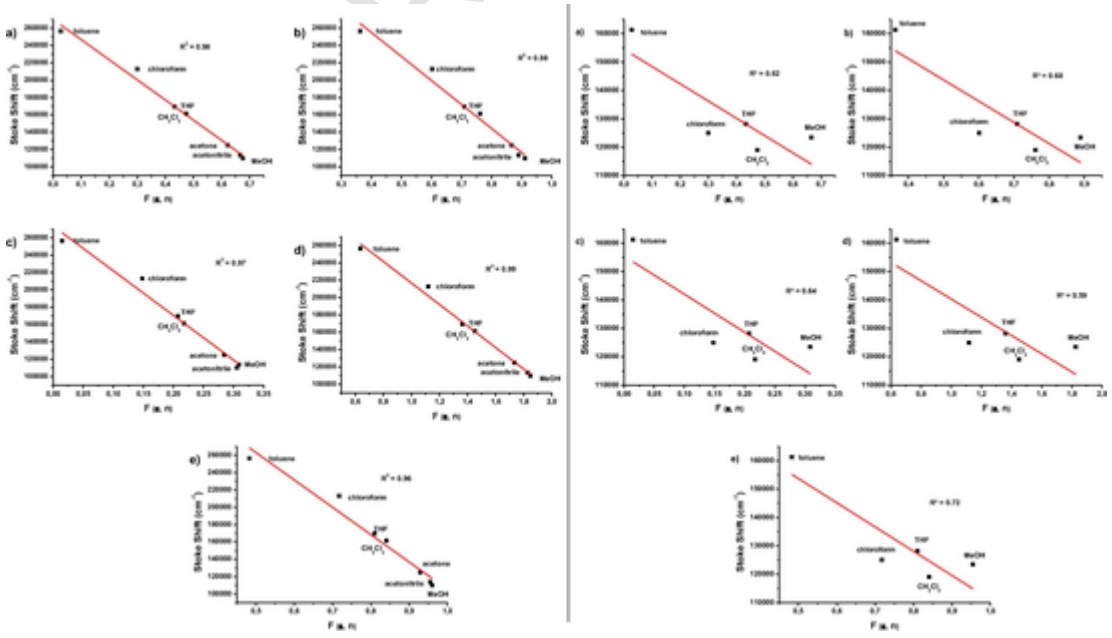

Fig. 5. Bakhshiev's (a), Kawski–Chamma–Viallet's (b), Lippert–Mataga (c), McRae's (d) and Suppan's (e) linear regressions for **PP1** and **PP2** in solvents of different polarities. Reproduced with permission from Tefhe et al. [150]. Copyright 2013 American Chemical Society.

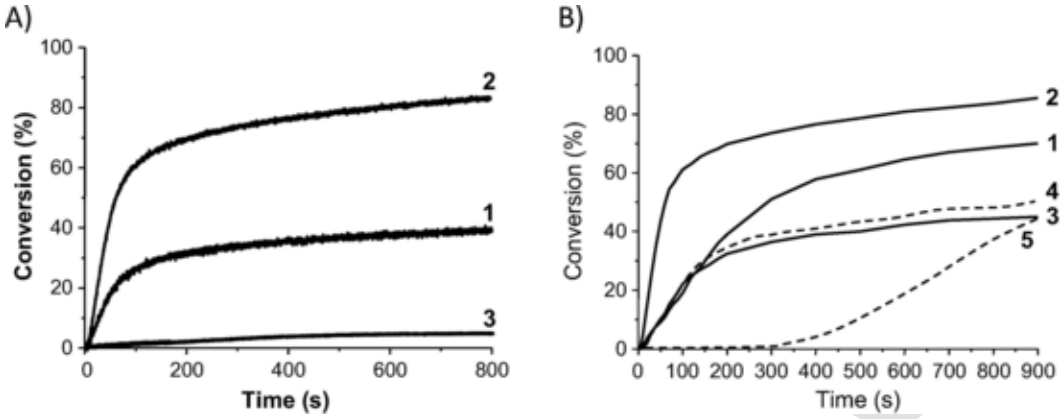

Fig. 6. A) Photopolymerization profiles of **EPOX** under air upon irradiation with a laser diode at 473 nm **1**) **PP1**/Iod (0.3%/2% w/w); **2**) **PP2**/NVK/Iod (0.3%/3%/2% w/w); **3**) PP**2**/NVK/Iod (0.3%/3%/2% w/w). B) Photopolymerization profiles of **EPOX** under air in the presence of **PP1**/NVK/Iod (0.3%/3%/2% w/w); upon irradiation at (**1**) 457 nm; (**2**) 473 nm; (**3**) 532 nm; (**4**) 635 nm; (**5**) 405 nm respectively. Reproduced with permission from Tefhe et al. [150]. Copyright 2013 American Chemical Society.

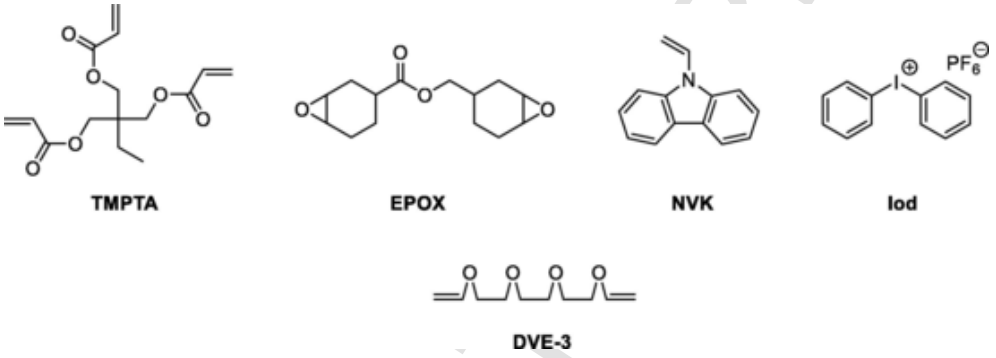

Fig. 7. The different monomers and additives used with **PP1** and **PP2**.

could be still detected with **PP2**, irrespective of the irradiation wavelength. Finally, the concomitant polymerization of EPOX and TMPTA at 473 nm in laminate was examined and an EPOX conversion of 40% and a TMPTA conversion of 70% could be respectively determined after 40 s, demonstrating the high reactivity of the three-component system. Interpenetrated polymer networks can thus be obtained with these three-component systems.

Investigation of the mechanism revealed the two-component **PPx**/Iod system to give rise to a fast photobleaching in solution upon excitation at 473 nm for **PP1** resulting from its oxidation by the iodonium salt. Conversely, no modification of the absorption spectrum could be detected for the two-component **PP2**/Iod system during the photolysis experiments, explained by a back-electron transfer regenerating **PP2** [163-166]. The higher efficiency of the three-component **PPx**/NVK/Iod system was assigned to the addition of the $Ph^{\bullet}$ radical onto NVK, generating the highly reactive Ph-$NVK^{\bullet}$ radical [73,167-171]. Formation of the two radicals $Ph^{\bullet}$ and Ph-$NVK^{\bullet}$ were confirmed by electron spin resonance (ESR) spin trapping (ESR-ST) experiments. Therefore, the following mechanism could be proposed to support the CP of EPOX and the FRP of TMPTA (See Fig. 8).

While elongating the spacer between the dimethylaminophenyl groups and the indane-1,3-dione acceptor, a red-shift of the absorption was clearly detected for **PP3**, with an ICT band extending from 400 to 650 nm [172]. The absorption maximum was detected at 532 nm with a molar extinction coefficient of 16200 $M^{-1}.cm^{-1}$. However, a lower reactivity was detected during both the FRP of TMPTA as no polymerization could be detected with the three-component **PP3**/MDEA/R – Br (0.3%/4%/3% w/w) system (where MDEA stands for *N*-methyldiethanolamine and R-Br for phenacyl bromide (See Fig. 9)) after 400 s of irradiation at 532 nm and only a weak conversion of 35%

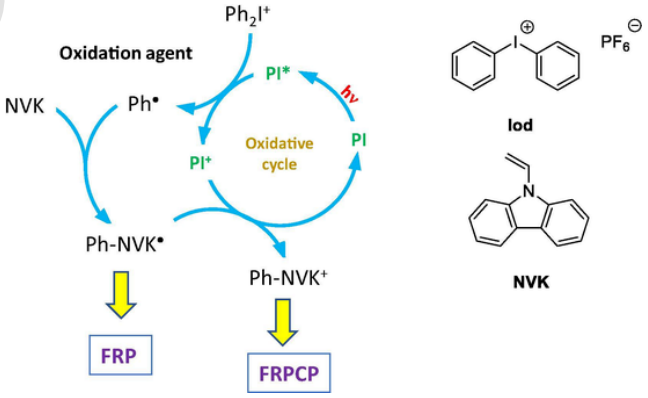

Fig. 8. Mechanism supporting the FRP of acrylates and the CP of epoxides.

could be determined for the CP of EPOX with the three-component system **PP3**/NVK/Iod2 (0.3%/3%/2% w/w) after 800 s of irradiation at 532 nm. This lack of reactivity was confirmed by the different photolysis experiments. Indeed, if a fast bleaching could be observed for its parent **PP1** with Iod (~4 min.), a 4-fold elongation of the reaction time was determined for the **PP3**/Iod2 system (~16 min.). Interestingly, examination of the EPOX films prepared with the three-component **PP3**/NVK/Iod2 (0.3%/3%/2% w/w) system revealed the radicals to be still detectable, even after several weeks, evidencing the exceptional stability of the radicals formed.

As mentioned in the introduction section, position of the ICT band of push–pull dyes can be finely tuned by modifying the electron donating ability of the donors and a relevant example of this was demonstrated with **PP4-PP7** (See Fig. 10) [173]. If tridecylbenzene (in **PP4**)

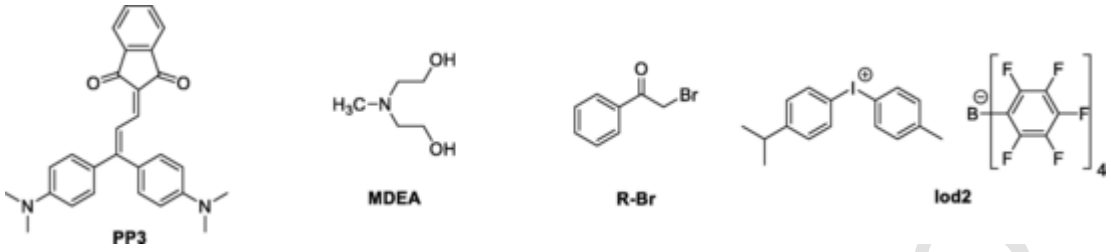

Fig. 9. Chemical structure of **PP3** and additives.

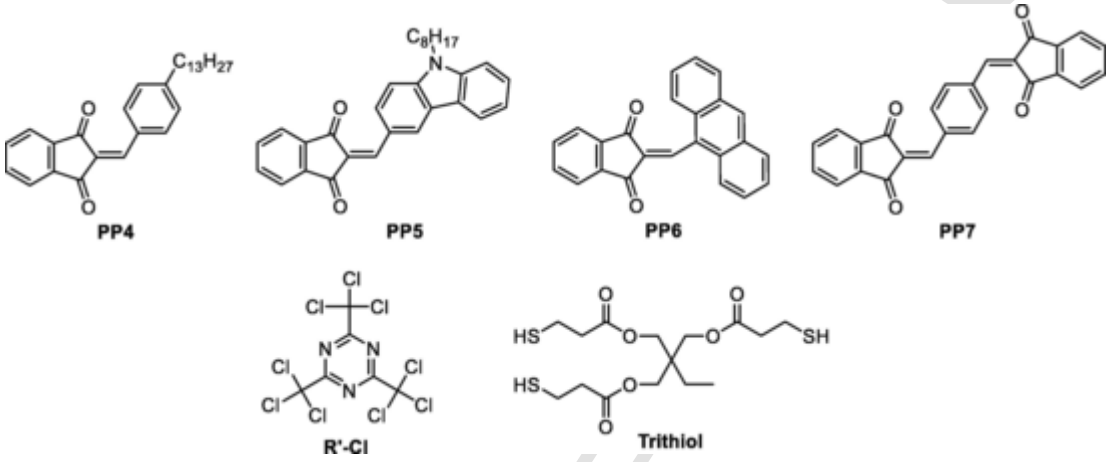

Fig. 10. Chemical structures of **PP4-PP7** and additives.

or benzene (in **PP7**) were weak electron donors so that the ICT bands of **PP4** and **PP7** were located in the 300–450 nm region (λ_{max} (**PP4**) = 351 nm, ε = 29900 $M^{-1}.cm^{-1}$, λ_{max} (**PP7**) = 389 nm, ε = 26900 $M^{-1}.cm^{-1}$), use of a strong electron donor such as carbazole redshifted the absorption maximum of **PP5** at 448 nm (ε = 42200 $M^{-1}.cm^{-1}$). Finally, by its polyaromatic structure, anthracene furnished the push–pull dye with the most redshifted absorption, the absorption maximum of **PP6** being located at 467 nm (ε = 7700 $M^{-1}.cm^{-1}$).

If the molar extinction coefficient of photoinitiators is an important parameter as its increase allows to drastically reduce the photoinitiator content, the solubility is another major issue which can adversely affect the polymerization efficiency [67,174]. This problem was confirmed with **PP7** that displayed a low solubility in the photocurable resin (EPOX, TMPTA) due to its extended planarity favoring π- π stacking interactions. Due to the lack of absorption at 457 nm, no polymerization could be done at this wavelength with **PP4** and **PP7**. Conversely, the absorption of **PP6** was insufficient so that no polymerization could also be carried out with this chromophore. Conversely, due to its absorption maximum at 448 nm, **PP6** was perfectly adapted for photopolymerization processes done with a laser diode at 457 nm (100 mW/cm^2) and a final monomer conversion of 59% was obtained for EPOX with the three-component system **PP5**/Iod/NVK (0.5%/2%/3%, w/w/w). While using a halogen lamp displaying a broader emission range (12 mW/cm^2, 370–800 nm), the low light intensity delivered by this lamp only allowed **PP5** to be efficiently in these mild conditions (64% monomer conversion after 800 s), followed by **PP7** (33% EPOX conversion after 800 s). Comparison with **PP1** revealed **PP4** to be more reactive in similar irradiation conditions (64% vs. 35% for **PP1** at 457 nm) whereas the benchmark photoinitiator camphorquinone was totally inefficient at this wavelength. When tested as the photosensitizer for the polymerization of TMPTA at 457 nm, three different three-component systems were identified as being efficient with **PP5**, namely **PP5**/Iod/NVK (0.5%/2%/3%, w/w/w), **PP5**/MDEA/R′−Cl (0.5%/2%/3%, w/w/w) and **PP5**/MDEA/R′−Cl (0.5%/2%/3%, w/w/w), furnishing monomer conversions of 58, 42 and 60% after 400 s respectively. Here again, the superiority of **PP5** over camphorquinone was confirmed, the highest monomer conversion peaking at 46% for the CQ/MDEA (0.5%/2%, w/w) combination. Excellent polymerization profiles could also be obtained for the dual polymerization of an EPOX/TMPTA blend or the thiol-ene reaction (See Fig. 11). Thus, tack free coatings could be obtained within 5 min for the EPOX/TMPTA blend under air and in laminate. However, the lower TMPTA conversion under air can be confidently assigned to oxygen inhibition, adversely affecting the FRP process. While examining the polymerization profiles of the trithiol/DVE-3 blend, the lower monomer conversion of trithiol (46% and 49% at 457 and 462 nm respectively) compared to DVE-3 (98% in both cases) was assigned to a concomitant and competitive cationic polymerization of DVE-3, improving its conversion. On the basis of ESR-ST, fluorescence, cyclic voltammetry, laser flash photolysis experiments, the following mechanism (r1-r4) could be proposed to support the thiol-ene polymerization reaction.

$$\mathbf{PP5} \rightarrow {}^{1}\mathbf{PP5}\ (h\nu) \text{ and } {}^{1}\mathbf{PP5} \rightarrow {}^{3}\mathbf{PP5} \quad \text{(r1)}$$

$$ {}^{1,3}\mathbf{PP5} + Ph_2I^+ \rightarrow \mathbf{PP5}^{\bullet +} + Ph_2I^{\bullet} \quad \text{(r2a)}$$

$$ \mathbf{PP5}^{\bullet +} + Ph_2I^{\bullet} \rightarrow \mathbf{PP5}^{\bullet +} + Ph^{\bullet} + Ph\text{-}I \quad \text{(r2b)}$$

$$ Ph^{\bullet} + NVK \rightarrow Ph\text{-}NVK^{\bullet} \quad \text{(r3a)}$$

$$ Ph\text{-}NVK^{\bullet} + Ph_2I^+ \rightarrow Ph\text{-}NVK^+ + Ph^{\bullet} + Ph\text{-}I \quad \text{(r3b)}$$

$$ Ph^{\bullet} + RS\text{-}H \rightarrow Ph\text{-}H + RS^{\bullet} \quad \text{(r4a)}$$

$$ RS^{\bullet} + R'\text{–}CH = CH_2 \rightarrow R'\text{–}CH^{\bullet}\text{-}CH_2SR \quad \text{(r4b)}$$

$$ R'\text{–}CH^{\bullet}\text{-}CH_2SR + RSH \rightarrow R'\text{–}CH_2\text{-}CH_2SR + RS^{\bullet} \quad \text{(r4c)}$$

The high reactivity of the **PP5**/MDEA/R′-Cl three-component system was supported by the highly negative free energy changes ΔG cor-

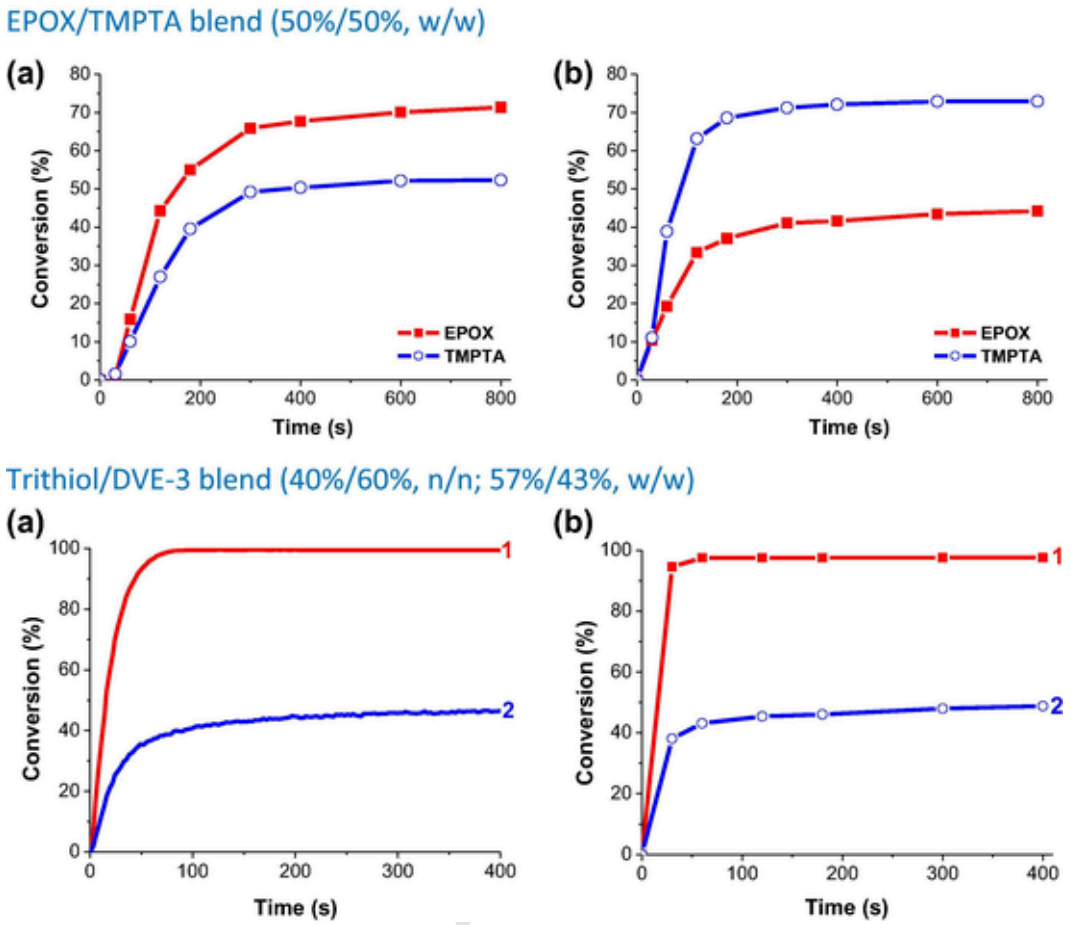

Fig. 11. Photopolymerization profiles of (top) an EPOX/TMPTA blend with **PP5**/Iod/NVK (0.5%/2%/3%, w/w/w) a) under air, b) in laminate (b) upon irradiation at 462 nm, (bottom) Trithiol/DVE-3 blend in laminate with **PP5**/Iod (0.5%/2%, w/w) upon irradiation (a) with a laser diode at 457 nm and (b) a LED at 462 nm. (1) DVE-3 conversion (2) trithiol conversion. Reproduced with permission from Xiao et al. [173]. Copyright 2014 American Chemical Society.

responding to an electron transfer reaction from MDEA to **PP5**. Also, the following mechanism could be proposed for the reaction involving the three-component **PP5**/MDEA/R′–Cl system (See Fig. 12).

A different behavior was found for the phenothiazine-based **PP8** that proved to be a poor photoinitiator in reductive initiating cycle [97]. Indeed, when combined with *N*-phenylglycine (NPG) as the amine, no photolysis could be detected for the **PP8**/NPG system (See Fig. 13). Conversely, a TMPTA conversion of 55% could be obtained with the **PP8**/Iod/NPG (0.2%/1%/1% w/w) upon irradiation at

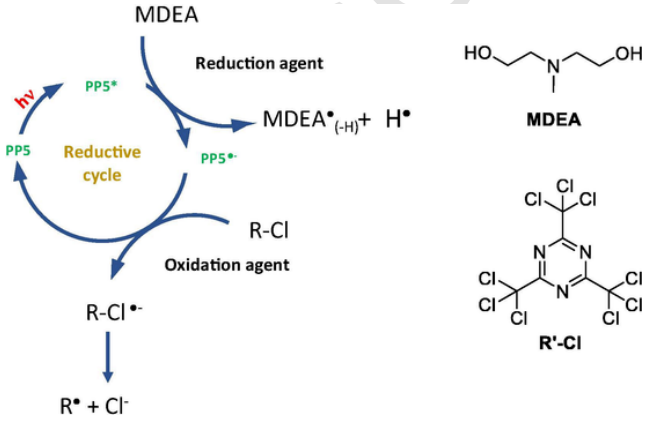

Fig. 12. Mechanism involved with the three-component **PP5**/MDEA/R′–Cl system.

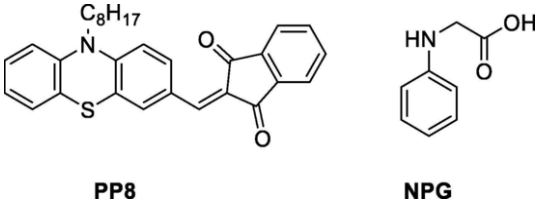

Fig. 13. Chemical structures of **PP8** and NPG.

405 nm. From these experiments, it was concluded that **PP8** was easier to oxidize than to reduce.

Finally, this year, a series of 21 push–pull dyes **PP9-PP29** was examined to establish a structure-performance relationship between two families of dyes differing by the polyaromaticity of the electron acceptors (See Fig. 14) [175].

It has to be noticed that contrarily to the previous works where only the commercially available indane-1,3-dione was used, in the present case, 1*H*-cyclopentanaphthalene-1,3-dione **EA1** and 2-(3-oxo-2,3-dihydro-1*H*-cyclopenta[*b*]naphthalen-1-ylidene)malononitrile **EA2** had to be prepared starting from naphthalene-2,3-dicarboxylic acid [127,176]. By esterification of the diacid with ethanol, the Claisen reaction of diethyl naphthalene-2,3-dicarboxylate with ethyl acetate and sodium hydride could provide after hydrolysis **EA1** in 91% yield for the two-steps. By mean of a Knoevenagel reaction with malononitrile, **EA1** could be converted as **EA2** in 67% yield.

The different dyes **PP9-PP29** could be prepared with reaction yields ranging from 74 to 94% yield, evidencing the efficiency of the Knoeve-

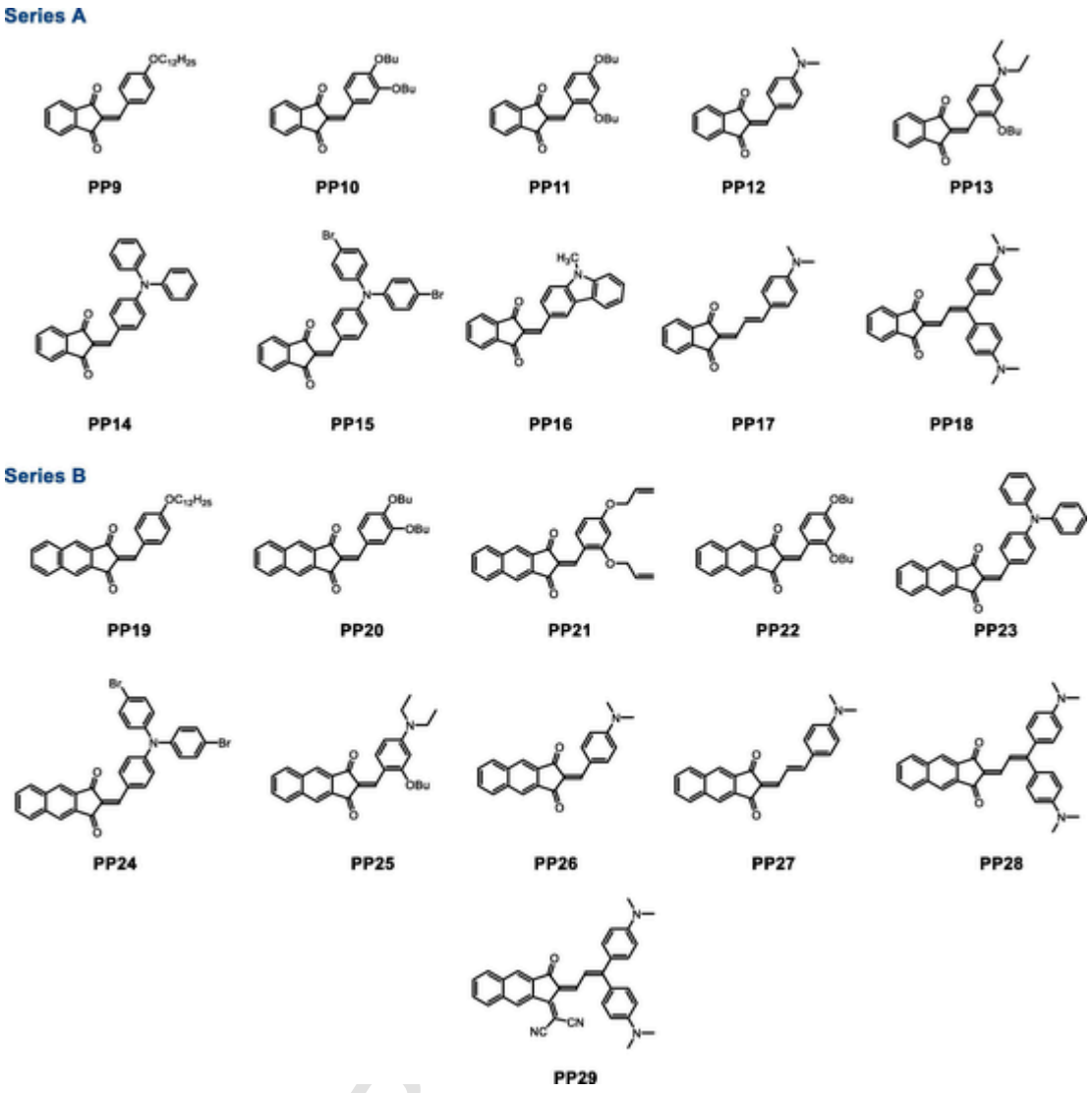

Fig. 14. Chemical structures of **PP9-PP29**.

nagel approach [126]. Considering that 10 different electron donors have been used, absorption maxima of the 21 dyes could range from 383 nm for **PP9** until 696 nm for **PP29** in acetonitrile (See Fig. 15). Interestingly, at similar electron donors, elongation of the electron acceptors resulted in a redshift of the absorption maxima by ca. 20 nm. Especially, by combining elongation of the π-conjugated spacer and extension of the polyaromaticity of the electron acceptor, a dye absorbing in the near infrared region could be even prepared (**PP29**).

Despites their huge differences concerning the absorptions of the 21 dyes, choice was done by the authors to test the different dyes only at

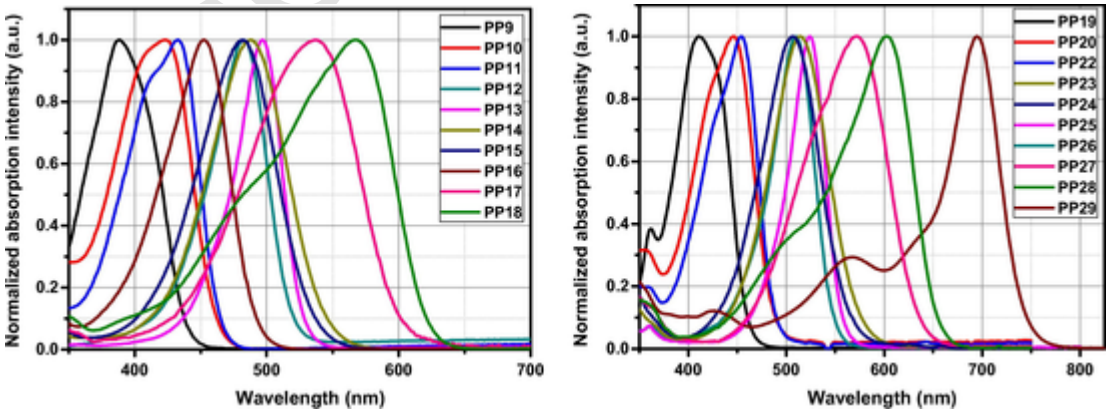

Fig. 15. Normalized UV–visible absorption spectra of **PP9-PP29** in dichloromethane. Reproduced with permission from Ref [126].

405 nm which is currently the wavelength under use in 3D printers [177-179]. Only their ability to induce the FRP of the tetrafunctional acrylate-based Ebecryl 40 was examined. Interestingly, monomer conversions obtained with the two-component systems dye/Iod (0.1%/2% w/w) remained low for this relatively reactive monomer, below 40%. Comparison with a reference photoinitiating system Iod3/ethyl dimethylaminobenzoate (EDB) revealed all the three-component systems **PPx**/Iod3/EDB (0.1%/2%/2% w/w) to outperform the reference system, except those prepared with **PP14**, **PP19** and **PP26**. Among the series, **PP13** and **PP25** were the most efficient, enabling to reach a final conversion higher than 90% within 50 s contrarily to 60% for the reference Iod/EDB system. Surprisingly, the best performances were obtained for the two dyes possessing the same electron donor, evidencing the crucial importance to examine a wide range of electron donors. As interestingly feature, a fast bleaching and formation of colorless coatings could be obtained with **PP13** whereas this highly researched property was not observed with **PP25**. Amon the 21 dyes, 10 of them could furnish final monomer conversions higher than 80%, namely **PP13**, **PP17**, **PP18**, **PP22-PP25**, **PP27-PP29**. Efficiency of the polymerization process is not only dependent of the molar extinction coefficients or the redox potentials of the photosensitizer. Another parameter of crucial importance is also the rate constant of interaction with the additives. In this field, photolysis of the **PP13**/Iod system could be realized within 5 min., far from those determined for **PP27** (25 min.) or **PP28** (50 min.). Parallel to this, **PP13** also showed a fast bleaching during photolysis of the **PP13**/EDB system. Therefore, it was concluded that the exceptional photoinitiating ability of **PP13** was related to its efficient interaction with the two additives so that a dual cure process could be proposed to support its superiority over the other dyes (See Fig. 16).

Due to its remarkable photoinitiating ability, some laser write experiments could be carried out with **PP13**, while using the three-component system **PP13**/Iod/amine (0.1%/2%/2% w/w/w) in Ebecryl 40, and well defined 3D-patterns could be obtained (See Fig. 17).

Finally, it has to be noticed that the use of indane-1,3-dione-based dyes was not limited to single-photon photopolymerization and that a few structures were also developed for two-photon polymerization (2PP). Chemical structures of the three dyes **PP30**, **PP31** [180] and **PP32** [181] used since 2015 are presented in the Fig. 18.

2.2. Push-pull dyes based on malononitrile and related derivatives

Malononitrile and its derivatives are relatively weak electron acceptors so that these electron acceptors are adapted for the synthesis of

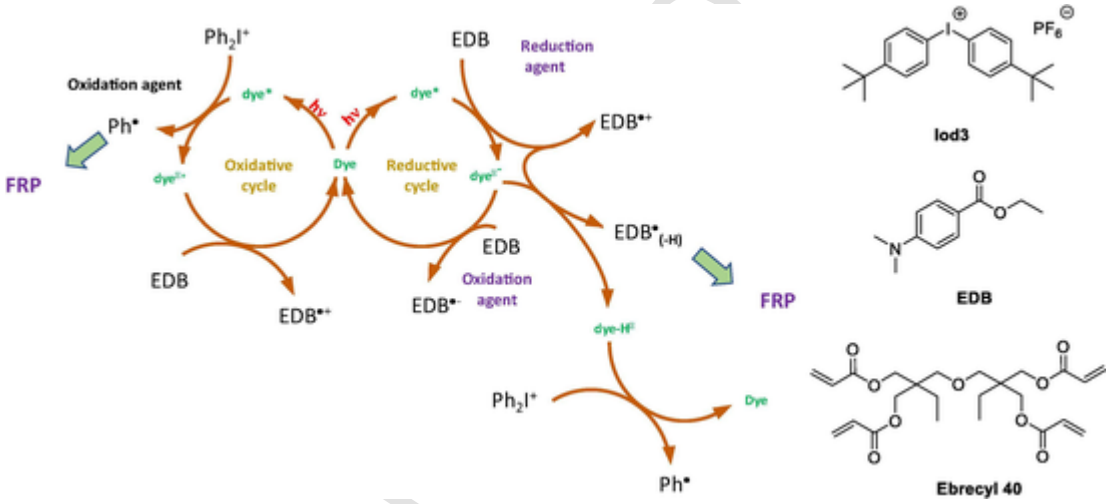

Fig. 16. Oxidative and reductive cycles involved in the FRP of Ebecryl 40 with **PP13**.

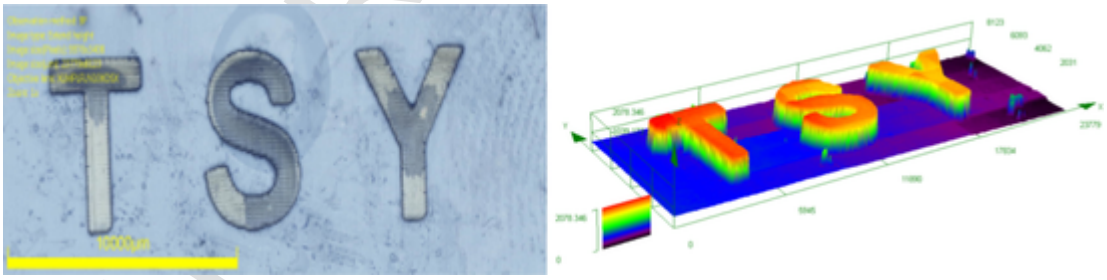

Fig. 17. 3D patterns obtained by laser write experiments using the three-component system **PP13**/Iod/amine (0.1%/2%/2% w/w/w) in Ebecryl 40. Reproduced with permission from Ref. [175].

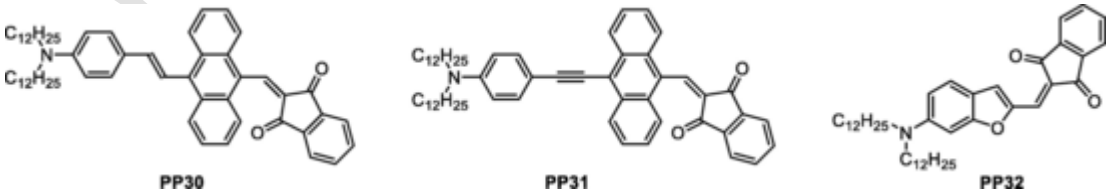

Fig. 18. Chemical structure of indane-1,3-dione-based dyes used in 2PP.

dyes absorbing in the 400–500 nm region. In 2013, a series of six dyes **PP33-PP38** exhibiting such an absorption has been reported by Lalevée and coworkers [182]. To determine the influence of the electron acceptors on the photoinitiating ability, two series of dyes were prepared, bearing malononitrile or dimethyl malonate as the electron acceptors (See Fig. 19). If the absorption maxima for **PP34**, **PP36** and **PP38** were found at 386, 374 and 366 nm respectively, a redshift of the absorption maxima of ca. 50 nm was found for all malononitrile-based dyes (428, 429 and 434 nm for **PP33**, **PP35** and **PP37** respectively).

Photolysis of the **PPx**/Iod systems revealed a fast bleaching to occur with **PP35** whereas no modification of the absorption spectra could be detected for the **PP33**/Iod and **PP37**/Iod systems. This behavior was assigned to a back-electron transfer from the $Ph_2I^{\bullet}$ radical to the oxidized dye $\mathbf{PPx}^{+\bullet}$, as already reported in the literature.[128,150,172] Polymerization efficiency of EPOX using a three-component system **PPx**/Iod/NVK (0.5%/2%/3% w/w) followed the trend previously established during the photolysis experiments, with **PP35** and **PP36** outperforming the four other dyes (50% monomer conversion after 1000 s of irradiation at 457 nm (100 mW/cm^2)). Therefore, it was concluded that the use of a strong electron donor (4-dimethylaminobenzene) was required to produce an efficient photoinitiator when using a weak electron-donor. In fact, the different experiments revealed **PP33** and **PP37** to lack of reactivity with Iod due to a back-electron transfer whereas the inefficiency of **PP34** and **PP38** was originating from their low absorptions. Finally, the best proof of the high reactivity of the **PP35**/Iod/NVK (0.5%/2%/3% w/w) was given during the polymerization of an EPOX/TMPTA blend (50%/50% w/w). While adding $AgSbF_6$, the FRP of TMPTA and the CP of EPOX could be both induced while simultaneously promoting the reduction of the silver salt, resulting in the formation of silver nanoparticles (See Fig. 20). In fact, the FRP of TMPTA and the reduction of the silver salt could be obtained thanks to the high reactivity of the Ph-NVK$^{\bullet}$ radicals, enabling the following radical oxidation process to occur :

$$\text{Ph-NVK}^{\bullet} + \text{Ag}+ \rightarrow \text{Ph-NVK}+ + \text{Ag}(0)$$

Elongation of the spacer in **PP39** enabled to redshift the absorption from ca **100** nm compared to that of **PP35**, at 532 nm (See Fig. 21) [173]. However, photolysis of the **PP39**/Iod combination revealed a slow interaction kinetic, what was confirmed by the polymerization experiments. Lastly, the disubstituted **PP40** was reported as an efficient photocatalyst to promote both the FRP of TMPTA or the BisGMA/TEGDMA mixture (which is extensively used in dentistry) [183-187]. or the CP of EPOX. For comparison, its monosubstituted analogue **PP41** was prepared (See Fig. 21) [97].

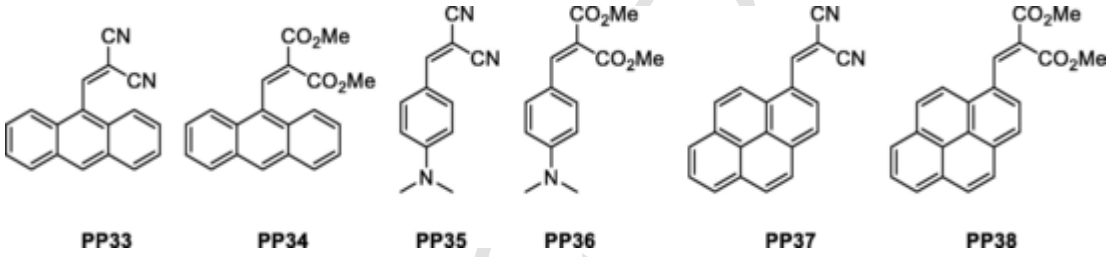

Fig. 19. Chemical structures of **PP33-PP38**.

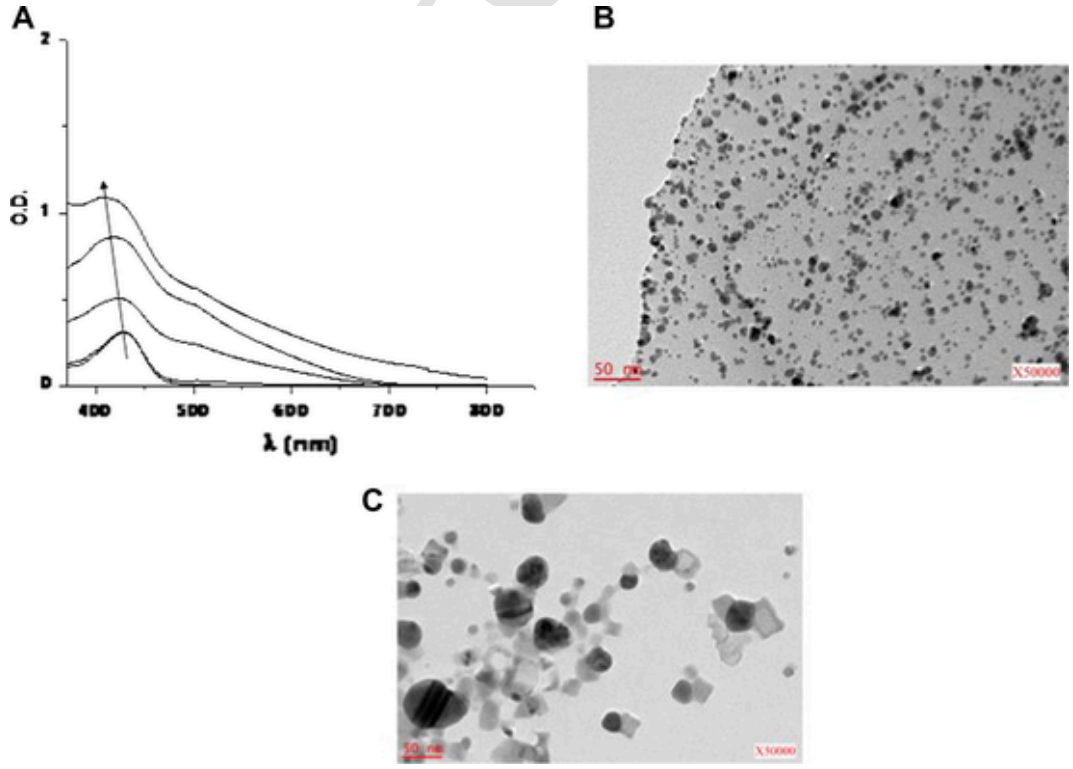

Fig. 20. STM micrographs of the silver nanoparticles formed during the polymerization of the EPOX/TMPTA blend with **PP35**. Adapted from Ref. [182] with permission from The Royal Society of Chemistry.

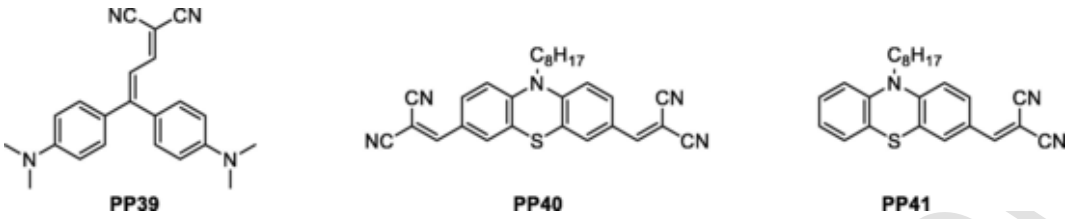

Fig. 21. Chemical structures of **PP39-PP41**.

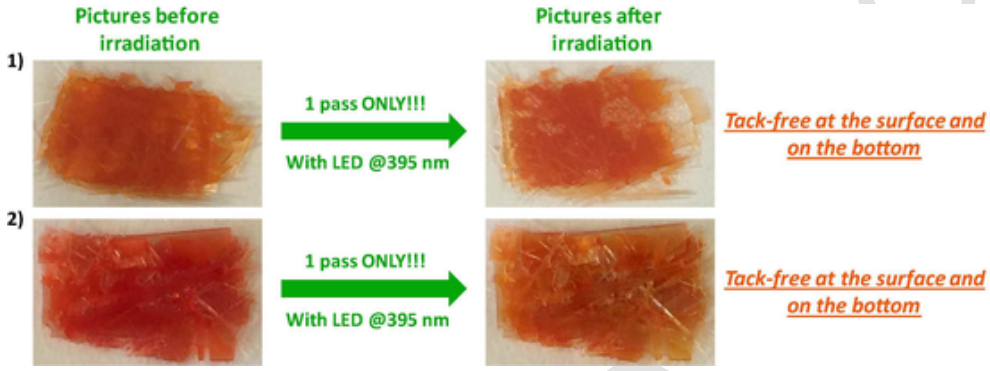

Fig. 22. Photocomposites obtained with a LED conveyor at 395 nm (belt speed : 2 m/min), using a glass fibers/(meth)acrylate resin (50%/50%) : (1) 0.05% **PP41** + 1% Iod + 1% NPG in BisGMA/TEGDMA; (2) 0.05% **PP40** + 1% Iod + 1% NPG in TMPTA. Adapted from ref. [97] with permission from The Royal Society of Chemistry.

Interestingly, **PP40** was already highly efficient in the two-component **PP40**/Iod (0.2%/1% w/w) system since a TMPTA conversion of 54% could be determined after 100 s of irradiation with a LED at 405 nm (110 mW/cm^2). Use of a three-component system **PP40**/Iod/NPG (0.2%/1%/1% w/w) did not significantly improved the monomer conversion, peaking at 56%. Conversely, an unusual behavior could be evidenced for **PP41**. Indeed, if **PP41** proved to be a moderate photoinitiator in two-component systems (46% of TMPTA conversion in the same conditions), a huge enhancement of the monomer conversion was obtained upon addition of NPG and a final conversion of 59% could be determined, outperforming **PP40**. This is directly related to the photocatalytic behavior of **PP41** which is efficiently regenerated by NPG in the three-component systems. Comparison with **PP8** also bearing a phenothiazine donor revealed the photoinitiating ability of **PP40**, **PP41** and **PP8** to be connected to both their absorption properties but also to the free energy changes (ΔGet) for the electron transfer with iodonium. Finally, the remarkable reactivity of **PP40** allowed the three-component system to be used for 3D printing experiments, but also to produce photocomposites. By impregnating the organic resin with 50% of glass fiber, tacking-free coatings could be obtained after only one pass in a LED conveyor at 395 nm with a belt speed of 2 m/min (See Fig. 22).

While using cyanoacetic acid as the electron acceptor, presence of the pH-sensitive group COOH on the dye can be advantageously used for the design of photobase generators [188]. This strategy was notably applied to the design of two photobase generators absorbing in the near-UV and visible-light range and differing by the counter-anions. In the literature, photobase generators absorbing in the near-UV/visible range and activable under low light intensity are still relatively scarce [189-200]. Besides, anionic polymerization provide a unique access to polymers that cannot be obtained by the traditional cationic or radical polymerization such as the epoxy/thiol or thiol/vinylsulfone copolymers [201]. From a synthetic viewpoint, these structures are relatively accessible since after preparation of the dye, addition of the appropriate base (1,8-diazabicyclo[5.4.0]undec-7-ene (DBU) or 1,5,7-triazabicyclo[4.4.0]dec-5-ene (TBD)) in the reaction media was sufficient to deprotonate the weak acid and provide the photobase generator (See Scheme 3). Photolysis experiments done in methanol upon irradiation with a LED at 385 nm (500 mW/cm^2) revealed the photolysis yield to remain low for **PP42**, around 0.04. However, even if this value is low, photolysis yield is consistent with those reported for other near-UV/visible photobase generators [202]. It has to be noticed that the working principle of photobase generators relies on a photoassisted decarboxylation of the chromophore, generating in situ a strong base that will subsequently deprotonate the protonated form of TBD or DBU (See Scheme 3).

When tested as photobase generators for the anionic polymerization of a trithiol/EPOX blend, higher monomer conversions and shorter reaction times were found for **PP43** upon irradiation at 385 nm, despite a lower photolysis yield (See Table 1). In this case, the enhanced reactivity of **PP43** was assigned to the release of a stronger base i.e. TBD (pKa = 26.0) vs. DBU (pKa = 24.3) for **PP42**.

2.3. Pyridinium-based dyes

Pyridinium group **A5** is among the most electron-withdrawing groups and its electron-withdrawing ability is comparable to that of tetracyanovinylindane **A2** [203-206]. Therefore, this group is appropriate for the design of visible-light photoinitiators. However, its cationic character which is inappropriate for numerous applications makes this electron accepting group, a less favorable candidate for the design of push–pull dyes. Concerning photopolymerization, a series of five molecules **PP44-PP47** was reported in 2013 by Lalevée and coworkers (See Fig. 23) [207].

As anticipated, use of this strong electron-acceptor enabled to prepare dyes absorbing between 350 and 600 nm and the highest molar extinction coefficient was determined for **PP45** (33 000 M^{-1} cm^{-1}) also known as DAST (dimethylaminostilbene) (See Fig. 24). Notably, this chromophore is extensively studied in nonlinear optical applications due to its remarkable molar extinction coefficient [208-214]. Considering the absorption spectra of **PP44-PP48**, the five dyes could be used as photoinitiators for polymerization processes done at 457 and 532 nm (See Table 2). If low monomer conversions could be determined for all two-component **PPx**/Iod systems used for the polymerization of EPOX upon irradiation with a halogen lamp (13 mW/cm^2, 350–800 nm), addition of *tris*(trimethylsilyl)silane (TMS)$_3$Si-H greatly improved the monomer conversions for **PP44** (50% vs. 0% within

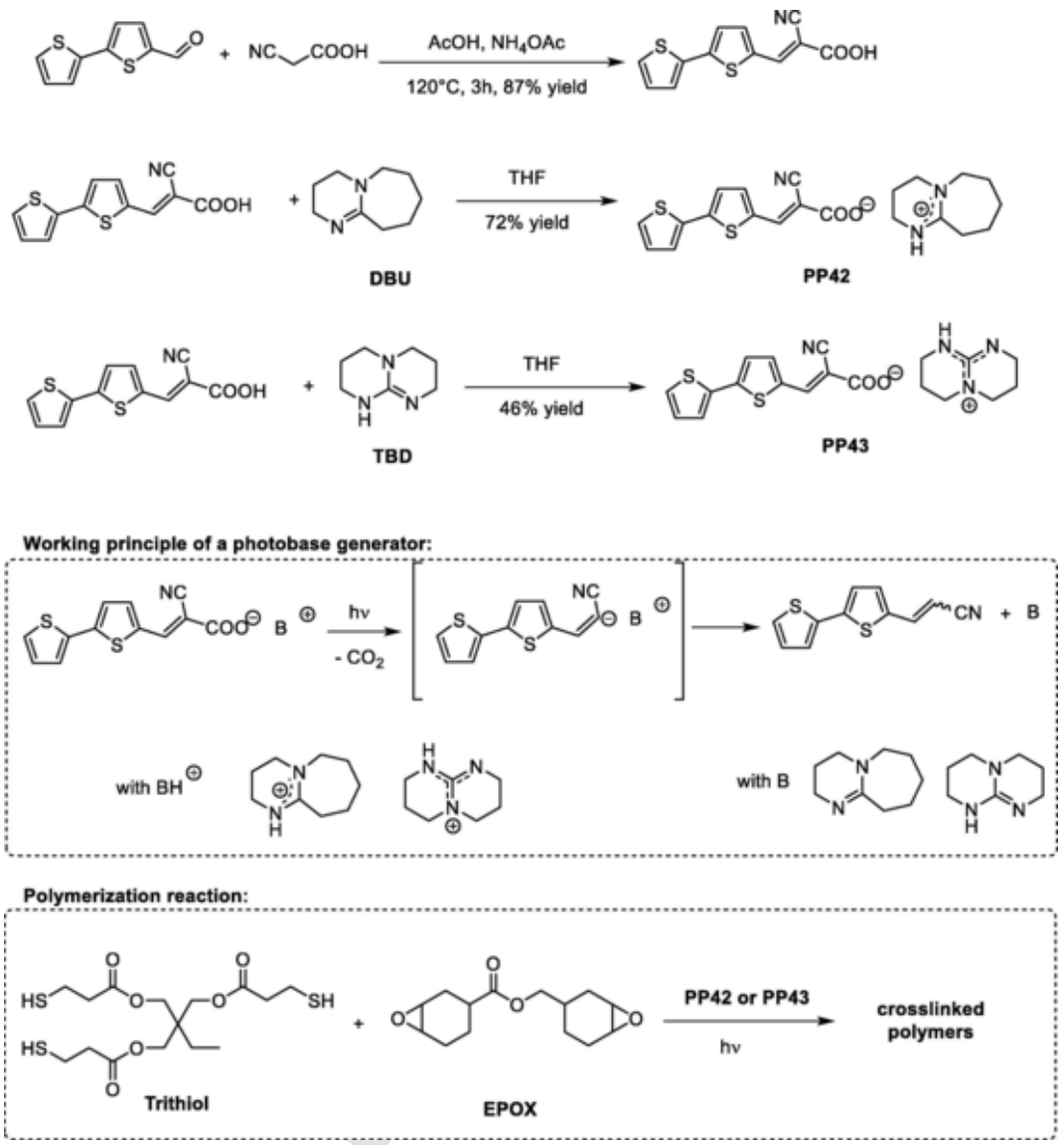

Scheme 3. Synthetic procedure to **PP42** and **PP43**.

Table 1
Monomer conversions upon irradiation for thiol/epoxy polymerizations.

PBG:	PP42 (6% wt)		PP43 (6% wt)	
Polymerization	Thiol/epoxy		Thiol/Epoxy	
Function	Thiol	Epoxy	Thiol	Epoxy
Time (min) @385 nm	90		49	
Conversion (%) @385 nm	67	65	90	75
Time (min) @405 nm	90			
Conversion (%) @405 nm	70	43		

1000 s), **PP45** (65% vs. 30% within 1000 s) or **PP46** (65% vs. 20% within 800 s) (See Fig. 25a). Unfortunately, all formulations prepared with **PP47** and **PP48** were unstable. The same holds true for **PP49** which was also unstable in the presence of an iodonium salt [172]. While examining the FRP of acrylates (TMPTA) upon exposure to laser diodes at 457 and 532 nm, a fast consumption of **PP44** and **PP45** could be monitored by FTIR with the three-component system **PPx**/$(TMS)_3Si–H/Ph_2I^+$ (0.2%/3%/2% w/w). As a result of this, the final TMPTA conversions remained low, peaking at 35%. As a significant advantage, colorless coatings could be obtained after polymerization. A monomer conversion approaching 45% could be determined with **PP46** in the same conditions. Good polymerization profiles were also obtained with **PP44** and **PP45** while using a photoreductive process with the two-component **PP44** or **PP45**/ MDEA (0.2%/5% w/w) systems (See Fig. 25b), the monomer conversion approaching 40%.

By ESR-ST experiments, the different radical species formed with the three-component **PPx**/$(TMS)_3Si–H/Ph_2I^+$ (0.2%/3%/2% w/w) and the two-component **PPx**/MDEA (0.2%/5% w/w) systems prepared with **PP44-PP46** could be identified so that the two mechanisms depicted in the Fig. 26 could be proposed.

Chemical structure of photoinitiators can drastically impact the photoinitiating ability. A relevant example of this was given for all dyes comprising Michler's aldehyde as the electron donor. If **PP49** was unstable in the presence of an iodonium salt, **PP50-PP52** proved also to be poor candidates for photoinitiation since no cationic polymerization of EPOX could be carried out with these structures (See Fig. 27). Conversely, **PP51** proved to be a relatively good photoinitiator for the FRP of acrylate and the three-component **PP51**/MDEA/R'-Cl (0.3%/4%/2% w/w) could outperform the reference camphorquinone/EDB (0.5%:2%,

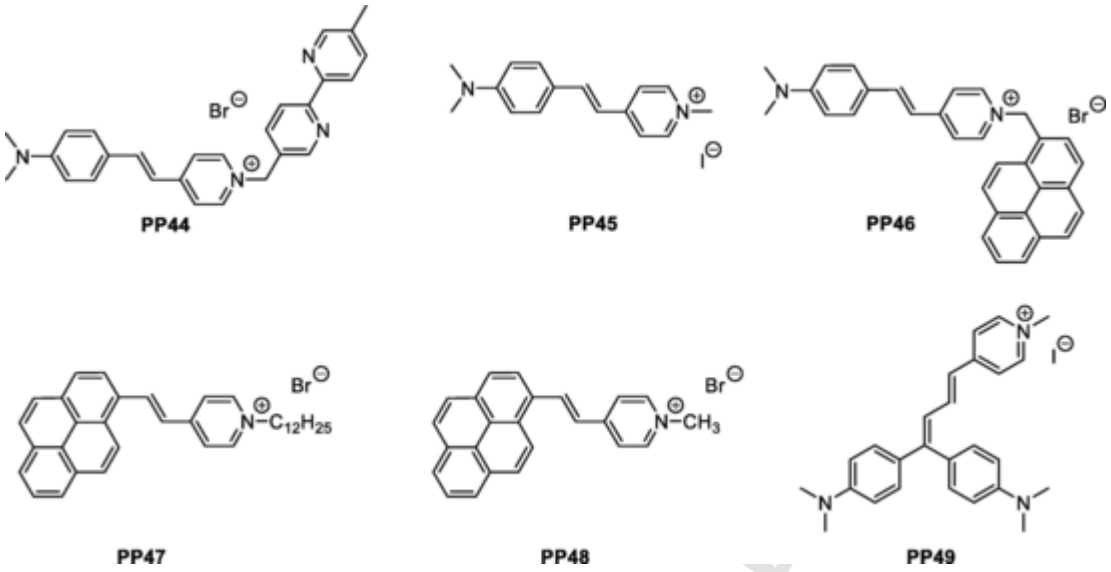

Fig. 23. Chemical structures of **PP44-PP49**.

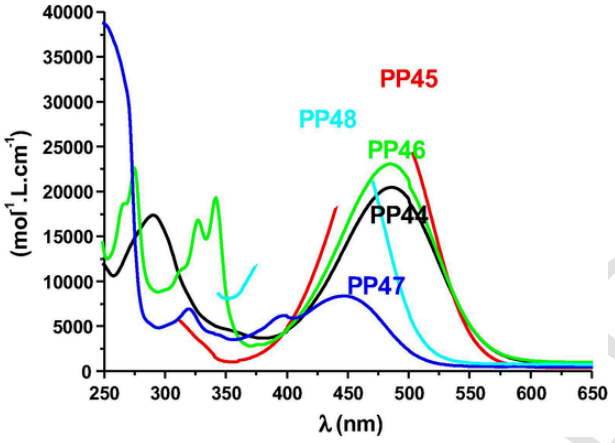

Fig. 24. UV–visible absorption spectra of **PP44-PP48**. Reprinted from Ref. [207], Copyright 2013, with permission from Elsevier.

w/w) system upon irradiation with a laser diode at 457 nm (55% vs 46% for the reference system).

2.4. Barbituric and thiobarbituric-based dyes

Michler's aldehyde is generally a poor candidate for the design of photoinitiators of polymerization as only mitigate results were reported with **PP18**, **PP28, PP39, PP50 and PP52**. However, this approach was more successful while using barbituric or thiobarbituric **EA3** derivatives as the electron acceptors (See Fig. 28). Indeed, the three-component **PP53**/NVK/Iod (0.3%/3%/2% w/w) system comprising **PP53** could efficiently initiate the CP of EPOX (65% of conversion after 800 s of irradiation at 532 nm with a laser diode) whereas low monomer conversions were determined for other Michler's based dyes in the same conditions (15% conversion for **PP54**, 35% for **PP3** or 18% for **PP39**) (See Fig. 29a).

Considering the broad absorption of **PP53**, this dye could also initiate efficient polymerizations at different excitation wavelengths, namely, 457, 473 and 532 nm (See Fig. 29b).

A similar efficiency was also observed during the FRP of TMPTA and the three-component system **PP53**/MDEA/R – Br (0.3%/4%/3% w/w) could furnish a final conversion of 55% upon irradiation at 532 nm, higher than that determined with **PP54** (35% yield), or **PP39** (25% conversion). Here again, the key element governing the reactivity of **PP53** was determined during the photolysis experiments done with the **PP53**/Iod and the **PP53**/MDEA combinations. In the two cases, a fast bleaching of the solutions was observed, faster than that determined for the **PP3-**, **PP39-** or **PP54**-based systems. In 2013, an interesting study was carried out on two push–pull dyes comprising a carbazole group as the electron donor. In this study, the difficulty which characterizes the development of push–pull dyes (**PP55** and **PP56**) as photoinitiators could be clearly evidenced [128]. Indeed, from their absorption viewpoint, the thiobarbituric derivative **PP56** exhibited only a slightly red-shifted absorption (λ_{max} = 460 nm in acetonitrile) compared to that of its barbituric analogue **PP55** (λ_{max} = 433 nm in acetonitrile). While examining their solvatochromic behavior using different empirical polarity scales, remarkable linear correlations could be obtained with the Bakhshiev' s, Lippert–Mataga, Kawski–Chamma–Viallet's, McRae's and Suppan's polarity scales for **PP56** whereas no reasonable linear relationships could be established for **PP55** (See Fig. 30).

The unexpected solvatochromic behavior of **PP55** was assigned to its ability to form dimers in solution as a result of hydrogen bond interactions. Parallel to this, ability of the solvents to interact with the electron acceptors and to induce the formation of mesomeric forms was suggested as promoting this irregular behavior in solution (See Fig. 31). Finally, an analogy was found in photopolymerization. Indeed, if **PP56** could efficiently promote the FRP of TMPTA and the CP of EPOX, photoinitiating ability of **PP55** was far behind that of **PP56**, suggesting that the photoinitiating ability of the push–pull dyes could be anticipated with regards to their solvatochromic behaviors. As shown in the Fig. 32, if a similar TMPTA conversion of 45% could be obtained with the three-component **PP56**/MDEA/R–Br (0.3%/4%/3% w/w) or the **PP56**/NVK/Iod (0.3%/3%/2% w/w) systems, no monomer conversion could be obtained with **PP55**, irrespective of the oxidative or the reductive conditions used. The same behavior was observed during the CP of EPOX, only **PP56** enabling to polymerize the monomer (55% for the three-component **PP56**/NVK/Iod (0.3%/3%/2% w/w) system).

2.5. Benzothiazole-based dyes

Benzothiazoles have been the focus of intense research efforts aiming at improving the production of initiating radicals. In this field, remarkable works have been reported by Kabatc and coworkers who developed three-component photoinitiating systems comprising a ben-

Table 2
Summary of the optical properties the different push–pull dyes discussed in this review.

Dye	λ_{max}(nm)	spectral range(nm)	photo-bleaching	Dye	λ_{max}(nm)	spectral range (nm)	photo-bleaching
PP1	478	350–550	no	**PP35**	429	350–500	no
PP2	464	350–750	no	**PP36**	374	275–450	no
PP3	558	350–650	no	**PP37**	434	350–525	no
PP4	351	300–450	no	**PP38**	366	300–450	no
PP5	448	350–525	no	**PP39**	500	350–600	no
PP6	467	400–550	no	**PP40**	489	375–600	no
PP7	389	–	no	**PP41**	463	375–600	no
PP8	494	400–650	no	**PP42**	387	325–475	no
PP9	388	350–450	no	**PP43**	387	325–475	no
PP10	423	350–480	no	**PP44**	495	400–600	**yes**
PP11	433	350–480	no	**PP45**	492	350–575	**yes**
PP12	483	350–540	no	**PP46**	496	400–600	no
PP13	497	400–550	**yes**	**PP47**	450	350–525	no
PP14	488	400–580	no	**PP48**	452	350–525	no
PP15	482	350–560	no	**PP49**	435	350–650	no
PP16	453	350–530	no	**PP50**	544	400–700	no
PP17	538	350–650	no	**PP51**	461	350–600	no
PP18	568	400–650	no	**PP52**	544	400–700	no
PP19	410	350–500	no	**PP53**	550	400–650	no
PP20	447	350–550	no	**PP54**	598	400–675	no
PP21	454	350–550	no	**PP55**	433	350–500	no
PP22	454	350–550	no	**PP56**	460	350–550	no
PP23	514	400–600	no	**PP57**	490	–	no
PP24	506	400–600	no	**PP58**	556	–	no
PP25	524	450–600	no	**PP59**	535	–	no
PP26	510	400–600	no	**PP60**	525	450–650	no
PP27	573	450–650	no	**PP61**	525	450–650	no
PP28	603	400–700	no	**PP62**	620	500–750	no
PP29	695	400–800	no	**PP63**	540	450–600	no
PP30	542	400–700	no	**PP64**	540	450–600	no
PP31	561	400–700	no	**PP65**	–	–	no
PP32	520	450–660	no	**PP66**	–	–	no
PP33	428	300–500	no	**PP67**	501	400–650	no
PP34	386	300–450	no	**PP68**	450	375–625	no

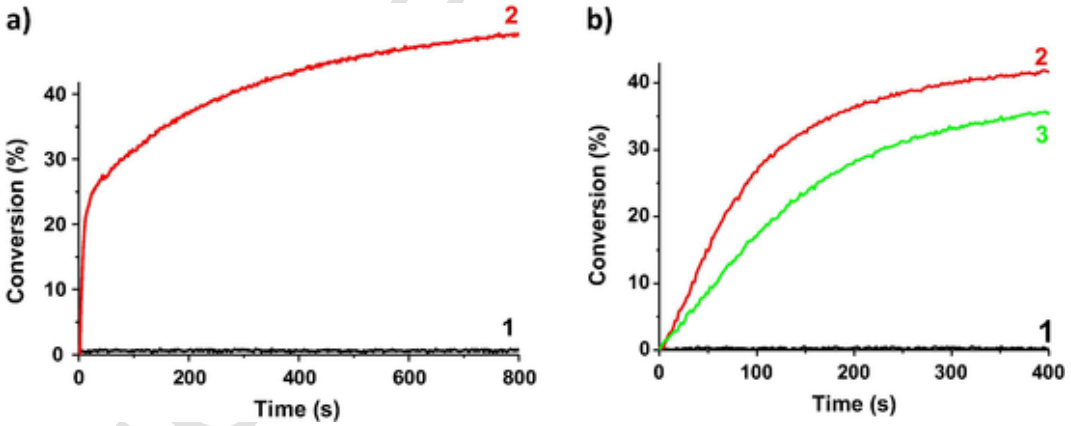

Fig. 25. Photopolymerization profiles of TMPTA upon irradiation with a halogen lamp in laminate in the presence of a) (1) **PP46**/Ph_2I^+ (0.2%/2% w/w); (2) **PP46**/$(TMS)_3Si$–H/Ph_2I^+ (0.2%/3%/2% w/w) b) **D_1** (0.2% w/w); (2) **PP44**/ MDEA (0.2%/5% w/w); (3) **PP44**/ MDEA (0.2%/5% w/w) upon irradiation with a laser diode at 532 nm. Reprinted from ref. [207], Copyright 2013, with permission from Elsevier.

zothiazole dye, a borate salt acting as a primary source of radicals and a 1,3,5-triazine derivative a secondary source of radicals [215]. Elucidation of the mechanism by fluorescence quenching experiments revealed the first reaction to consist in an electron transfer from the dyes (**PP57-PP59**) to the borate salt and in a second step, the resulting dye radical to subsequently react with the triazine derivative, inducing a carbon-halogen bond cleavage and producing a triazine radical, concomitantly regenerating the dye (See Scheme 4).

As the secondary source of radicals, pyridinium salts were also examined, demonstrating a similar efficiency than that of the triazine derivatives [216]. A few examples of pyridinium co-initiators are presented in the Scheme 5, and the cleavage mechanism involved in the

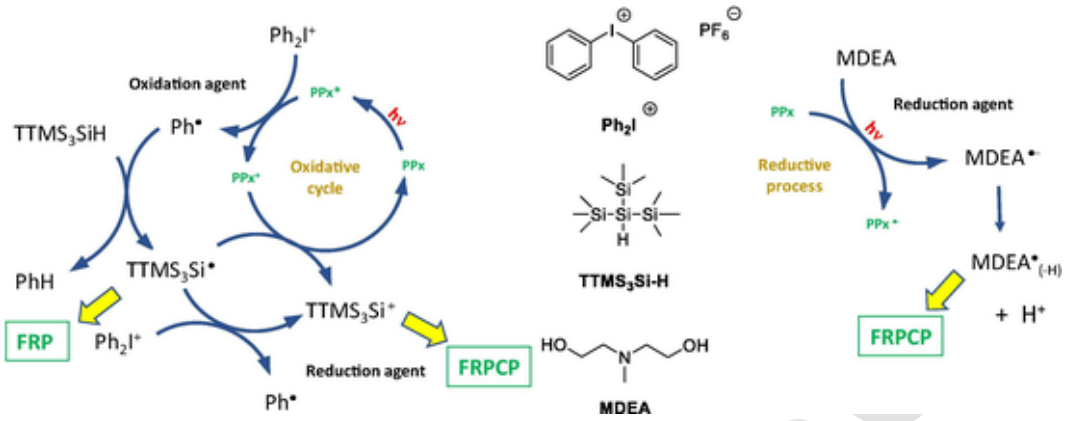

Fig. 26. Mechanism supporting the photoinitiation process with **PP44-PP46**.

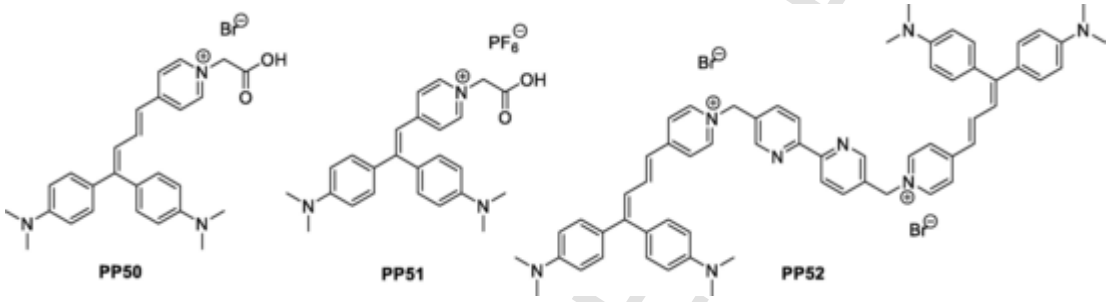

Fig. 27. Chemical structures of **PP50-PP52**.

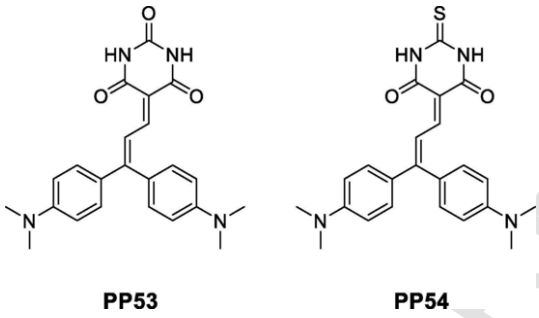

Fig. 28. Chemical structures of **PP53** and **PP54**.

production of pyridinium radicals is also provided. Over the years, the number of three-component systems comprising a benzothiazole dye, a borate salt and a co-initiator drastically increased and 2-mercaptobenzoxazole, 2-mercaptobenzothiazole, 2-mercaptobenzimidazole or 2-methyl-1,3-dioxolan were respectively examined as potential co-initiators for dye/borate systems [217]. In 2015, the same authors went a step further by covalently linking the secondary source of radicals to the dye (See **PP60-PP62**) [218]. Using this strategy, the extractability issue could be efficiently addressed by reducing the migratability of small molecules within the polymer network. This point is of crucial importance, especially for food and biological applications [12,219,220]. Additionally, from an industrial point of view, a simplification of the photocurable resins can be obtained, only requiring the

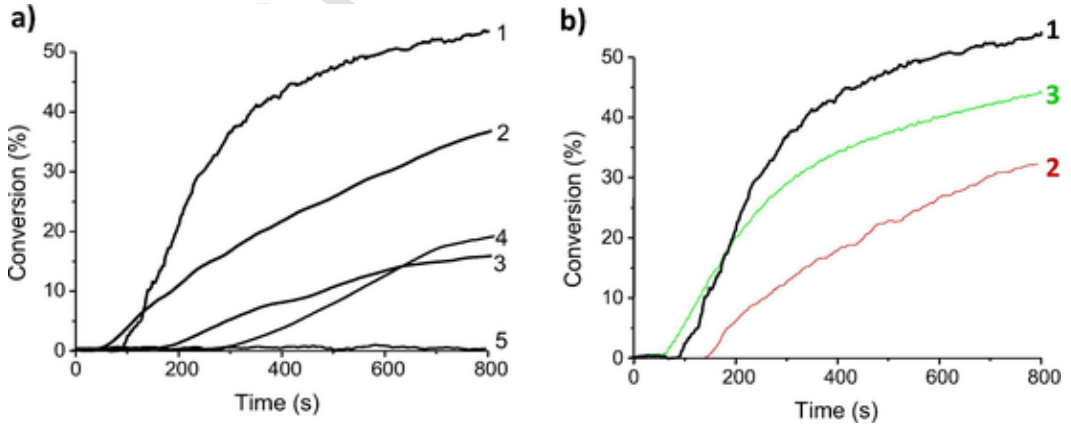

Fig. 29. Photopolymerization profiles of EPOX under air. a) Upon irradiation with a laser diode at 532 nm (**1**) **PP53**/NVK/Iod (0.3%/3%/2% w/w); (**2**) **PP3**/NVK/Iod (0.3%/3%/2% w/w); (**3**) **PP54**/NVK/Iod (0.3%/3%/2% w/w); (**4**) **PP39**/NVK/Iod (0.3%/3%/2% w/w); (**5**) Michler's aldehyde/NVK/Iod (0.3%/3%/2% w/w). b) upon irradiation of the three-component system **PP53**/NVK/Iod (0.3%/3%/2% w/w) using laser diodes at (1) 532 nm; (2) 457 nm; (3) 473 nm Reproduced with permission from Tehfe et al. [172]. Copyright 2013 American Chemical Society.

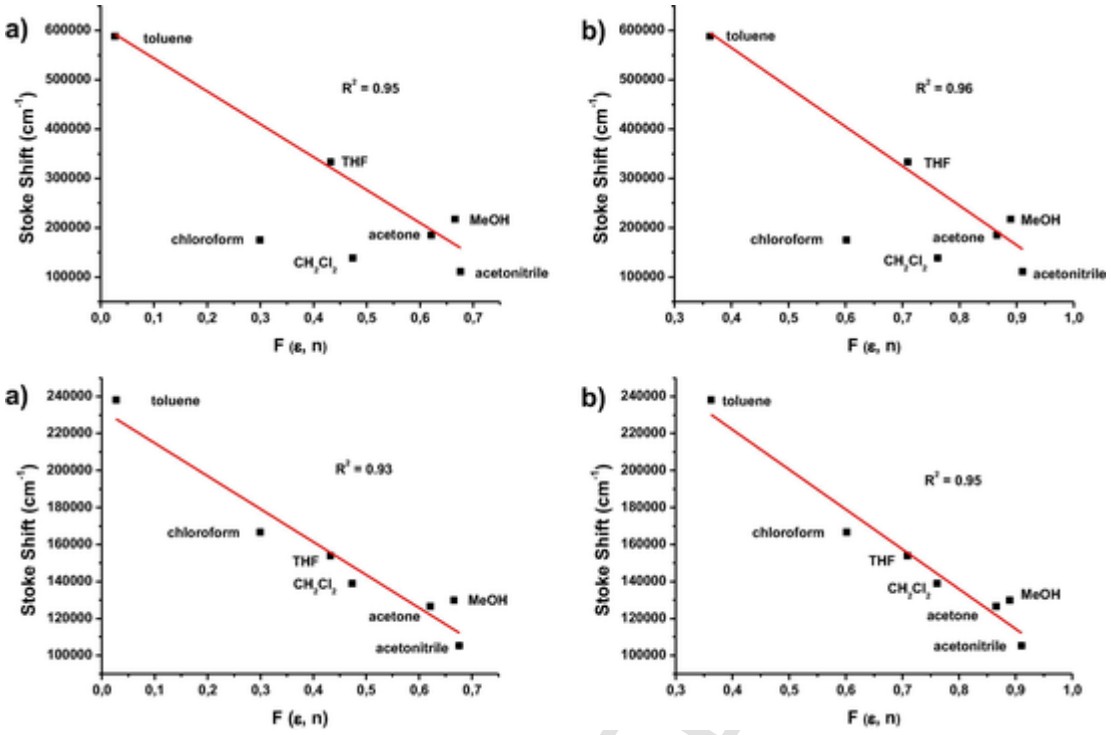

Fig. 30. Bakhshiev's (a), Lippert–Mataga (b), solvatochromic correlation plots for **PP55** (top) and **PP56** (bottom) in seven solvents of different polarities Adapted from Ref. [128] with permission from The Royal Society of Chemistry.

dye and the borate salt to be mixed together, the secondary source of radicals being covalently linked to the dye.

Interestingly, **PP60-PP62** exhibited a broad absorption over the visible range, extending from 450 to 650 nm for **PP60** and **PP61**, from 500 to 750 nm for **PP62**. In this context, photopolymerization of TMPTA could be examined at 514 nm for the three dyes (See Fig. 33). Among the three dyes, **PP62** proved to be the less efficient compound of the series, irrespective of the borate salts **B1-B4** used (See Fig. 34).

Conversely, final monomer conversions around 25% could be obtained with **PP61** in combination with the borate salts **B3** and **B4**. On the opposite, a low monomer conversion could be determined with **PP60** (~10%) whereas no polymerization could be obtained with the symmetric **PP62.** Interestingly, as previously reported for **PP55** and **PP56**, excellent linear regressions could be plotted for **PP60** and **PP61** while using the Lippert-Mataga's, Bakhshiev's, Kawski-Chamma-Viallet's, McRae's and Suppan's polarity scales. On the opposite, no reasonable correlation could be established with the Reichardt [152] or the Kamlet-Taft [153] polarity scales, what is perfectly consistent with the trend previously observed for **PP55** and **PP56**. Indeed, for these two dyes, no acceptable correlations could also be established with these two solvent polarity scales. Kabatc and coworkers also compared the photoinitiating ability of **PP60** and **PP61** with that of **PP63** and **PP64** which differ by the substitution patterns of the arylamino group for the FRP of TMPTA [221,222]. By replacing the dimethylamino group in **PP60** and **PP61** by a pyrrolidine group in **PP63** and **PP64**, a 3-fold reduction of the TMPTA conversion could be determined upon irradiating the resins with a laser emitting at 514 nm for 7 min. Here again, the low photoinitiating ability of **PP63** and **PP64** could be anticipated by examining their solvatochromic behavior in solution. Contrarily to **PP61** and **PP62** for which linear correlations could be established with the Lippert-Mataga's, Bakhshiev's, Kawski-Chamma-Viallet's, McRae's and Suppan's polarity scales, no reasonable correlations could also be established for **PP63** and **PP64**.

While using **PP59** as the reference compound, a few benzothiazole compounds could outperform this dye, as exemplified with **PP65** [223] or **PP66** [224] (See Fig. 35).

2.6. Pyran-based dyes

2-(2-(*tert*-Butyl)-6-methyl-4*H*-pyran-4-ylidene)malononitrile is a well-known electron-acceptor that was extensively used for the design of light-emitting materials for OLEDs [225,226]. In this field, the most popular compound is undoubtedly 4-(dicyanomethylene)-2-*tert*-butyl-6-(1,1,7,7-tetramethyljulolidin-4-yl-vinyl)-4*H*-pyran (DCJTB, **PP67**) which is a red fluorescent singlet emitter.[227-230] Considering its broad absorption extending from 400 to 600 nm, photoinitiating ability of DCJTB **PP67** was studied at 532 nm [231]. It has to be noticed that DCJTB is used in Organic Electronics, meaning that this compound exhibit reversible redox properties. Otherwise, it could not be used in devices. When tested as photoinitiators, similar final monomer conversion could be obtained for the polymerization of TMPTA using the three-component **PP67**/Iod/NVK (0.5%/2%/3%, w/w/w) or **PP67**/MDEA/R′-Cl (0.5%/2%/1%, w/w/w) systems. Thus, a monomer conversion of 41% and 57% were respectively determined with these two systems upon irradiation at 532 nm for 400 s (See Fig. 36). These results are much higher than that of the reference system based on camphorquinone (CQ). In this last case, conversions of 18 and 35% were respectively obtained with the two-component CQ/Iod and CQ/MDEA systems. High final monomer conversions could also be obtained during the CP of EPOX, peaking at 70% for the DCJTB/Iod/NVK (0.5%/2%/3%, w/w/w) upon irradiation with an halogen lamp or by irradiation with laser diodes emitting at 473 and 532 nm.

Here again, the high efficiency of **PP67** was determined by fluorescence quenching experiments and a high rate constant of interaction could be measured in solution for **PP67**/Iod (6.0×10^9 $M^{-1}.s^{-1}$) which was determined as being diffusion-controlled.

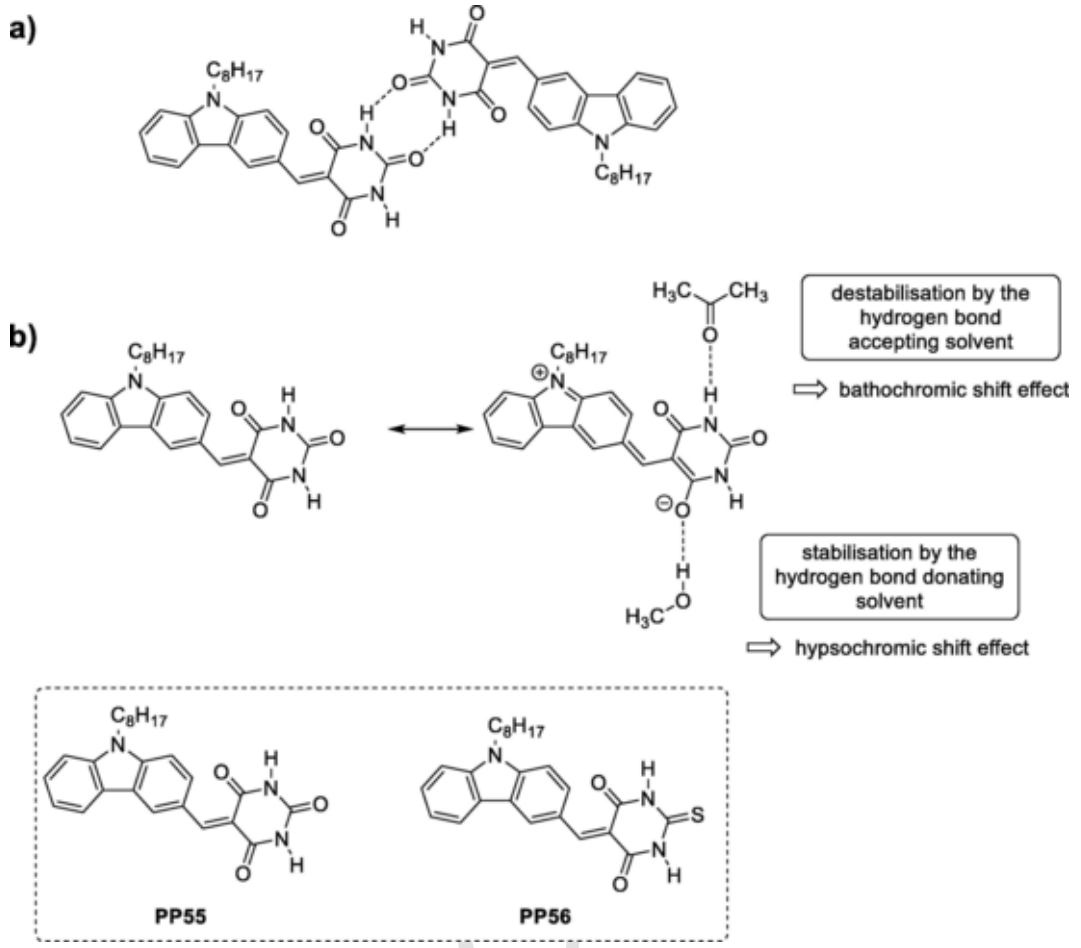

Fig. 31. Solvent effects influencing the solvatochromism of **PP55** in solution and chemical structures of **PP55** and **PP56**.

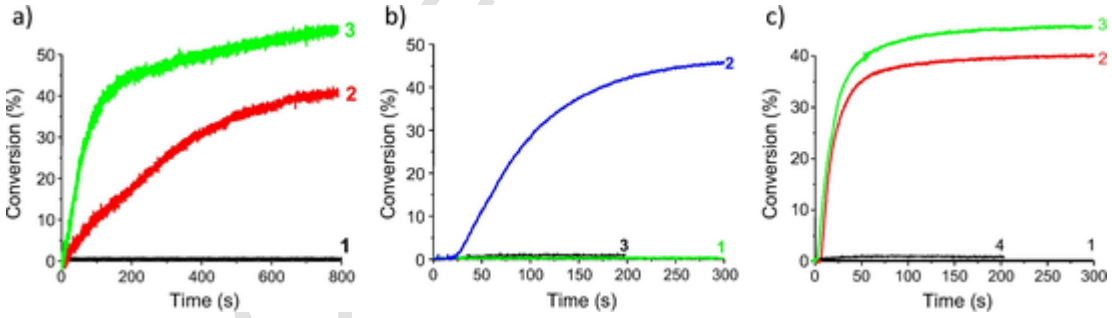

Fig. 32. a) Photopolymerization profiles of EPOX upon a laser diode irradiation at 473 nm under air in the presence of (**1**) **PP55**/NVK/Iod (0.3%/3%/2% w/w); (**2**) **PP56**/Iod (0.3%/2% w/w); (**3**) **PP56**/NVK/Iod (0.3%/3%/2% w/w); b) Photopolymerization profiles of TMPTA upon a laser diode irradiation at 473 nm in laminate in the presence of (**1**) **PP56**/ Iod (0.3%/2% w/w) and (**2**) **PP56**/NVK/Iod (0.3%/3%/2% w/w); (**3**) **PP55**/NVK/Iod (0.3%/3%/2% w/w); c) Photopolymerization profiles of TMPTA upon a laser diode irradiation at 473 nm in laminate in the presence of (**1**) **PP56**/R-Br (0.3%/3% w/w); (**2**) **PP56**/MDEA (0.3%/4% w/w); (**3**) **PP56**/MDEA/R-Br (0.3%/4%/3% w/w); (**4**) **PP55**/MDEA (0.3%/4% w/w). Adapted from Ref. [128] with permission from The Royal Society of Chemistry.

2.7. Rhodanine-based dyes

Rhodanine is a weak electron acceptor which is more and more used for the design of chromophores for organic solar cells. Indeed, rhodamine is an electron acceptor whose substitution can be easily carried out and numerous derivatives have been designed, comprising an acetic acid linkage. As a result of this specific substitution, a good anchorage of the dyes onto the surface of the TiO_2 electrode can be obtained in solar cells [232-236]. With respect to the use of rhodanine dyes as photoinitiators, to the best of our knowledge, only one dye has been reported at present, i.e. **PP68** (See Fig. 37) [97].

However, as the first candidate examined for photopolymerization, **PP68** proved to be a photoinitiator of moderate efficiency, being less efficient than photoinitiators such as **PP8**, **PP40** and **PP41**. Indeed, if final monomer conversion of 59, 55 and 56% could be determined for **PP41**, **PP8** and **PP40** respectively for the FRP of TMPTA upon irradiation with a LED at 405 nm in laminate, the monomer conversion decreased to 33% after 100 s of irradiation for the three-component systems **PP68**/Iod/NPG (0.2%/1%/1% w/w). An opposite trend was found for the CP of EPOX under air, the conversion of 58% being ob-

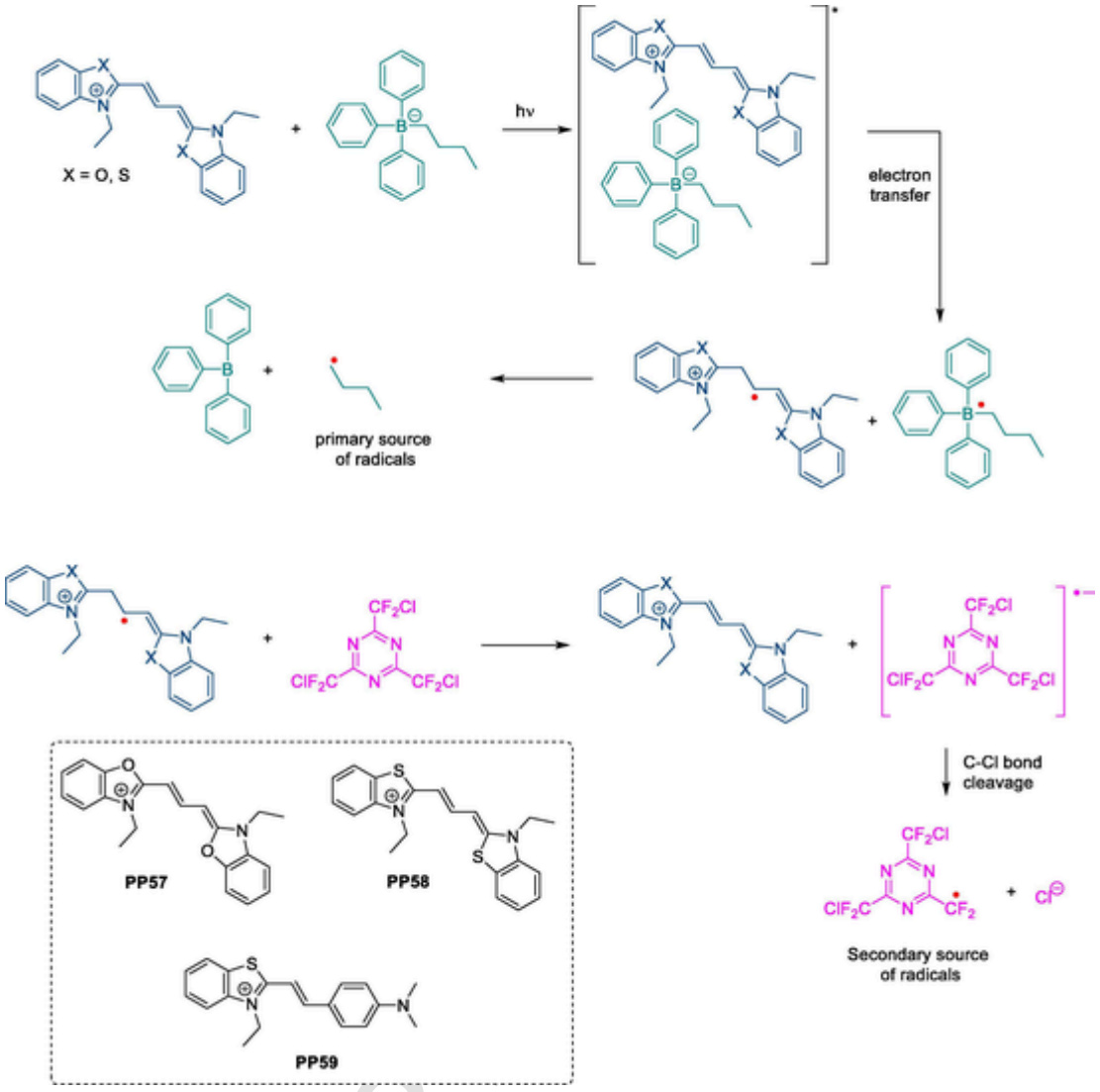

Scheme 4. Mechanism of radical production with **PP57-PP59**.

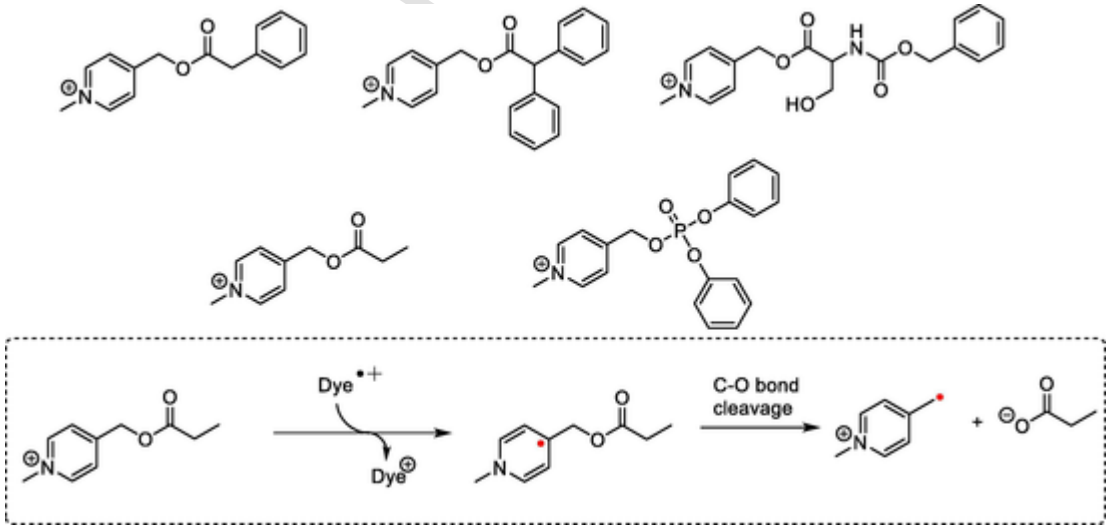

Scheme 5. examples of co-initiators used with benzothiazole-based dyes.

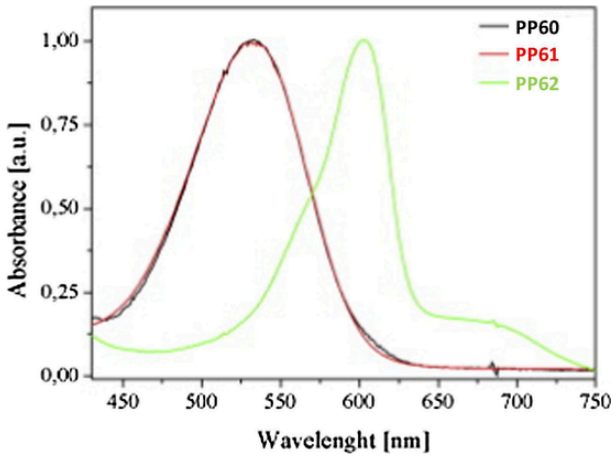

Fig. 33. UV–visible absorption spectrum of **PP60-PP62**. Reprinted from Ref. [218], Copyright 2015, with permission from Elsevier.

tained for the two-component **PP68**/Iod (0.5%/1% w/w) upon irradiation at 405 nm for 800 s outperforming that of **PP41**, **PP8** and **PP40** (57, 53 and 43% respectively).

2.8. Disadvantages of existing dyes and future prospects.

As mentioned in this review, push–pull dyes are excellent candidates for photoinitiation due to the possibility to finely tune the absorption spectra. These dyes are characterized by high molar extinction coefficients, what constitutes an appealing feature for photopolymerization by the possibility to reduce the photoinitiator content. However, a major drawback remains i.e. the color which is imposed by the photoinitiator to the resulting films. Among the 68 dyes presented in this review, this drawback has clearly been established since only three of them are capable to bleach i.e. to decompose so that colorless coatings can be obtained. In this field, one option could consist in developing push–pull dyes with weak donors and acceptors so that the intramolecular charge transfer band could be located in the near UV/visible range, addressing the color issue. As a second drawback of push–pull dyes as photoinitiators is their irregular ability to initiate a polymerization process. In this field, the relationship between solvatochromism and photoinitiating ability has been demonstrated. However, at present, this unexpected has not been rationalized yet by the different groups that worked on these structures. From a synthetic viewpoint, this is a major disadvantage since it can imply the synthesis of numerous dyes that will not work.

Concerning the future applications of push–pull dyes in photopolymerization, a few applications have already been examined such as 3D printing or laser writing applications. By using strong electron donors and acceptors, ICT bands of corresponding dyes could be red-shifted until the near infrared region so that the scope of applications of photopolymerization could be extended to the polymerization of filled samples and the elaboration of thick coatings, what is not achievable for photopolymerization processes done in the UV range [237,238]. As final applications that could emerge in the Future for polymer films con-

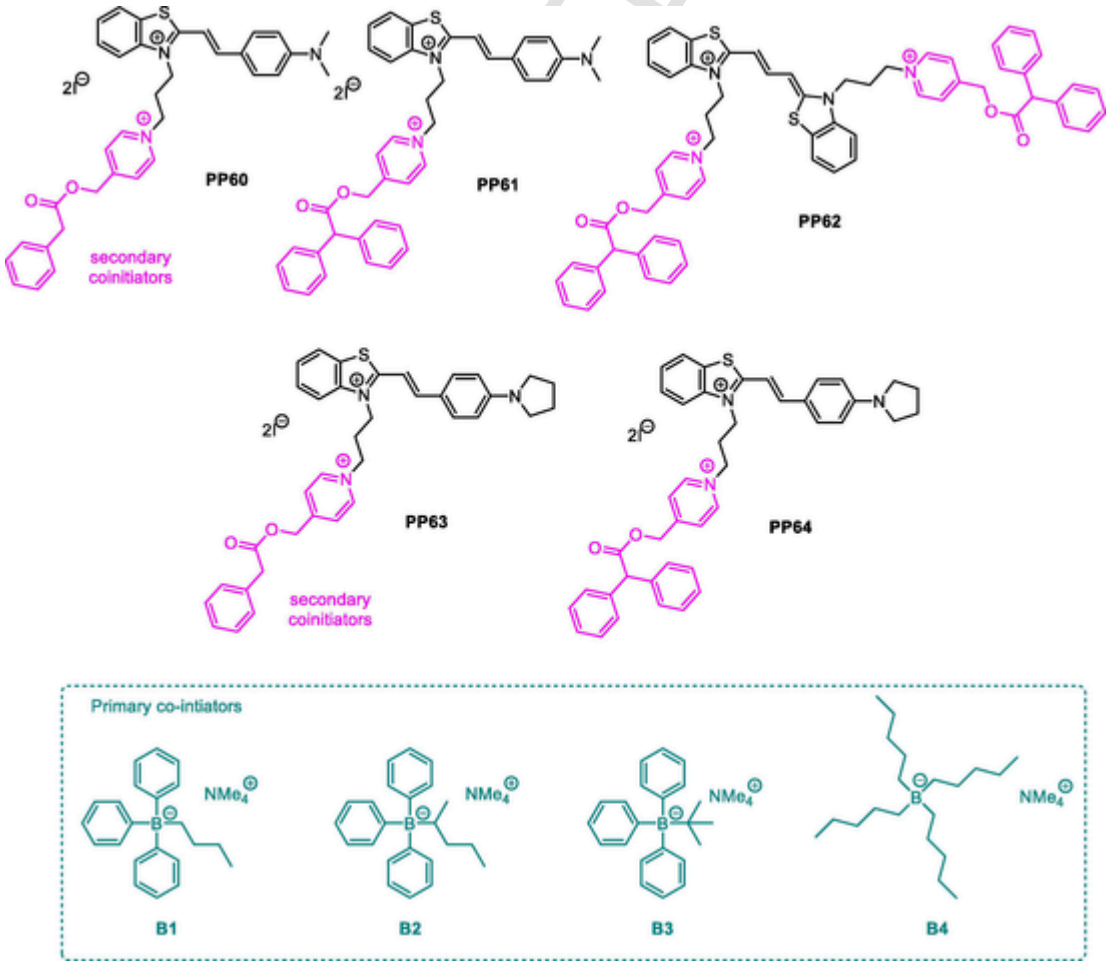

Fig. 34. Chemical structures of **PP60-PP64** and various borate salts.

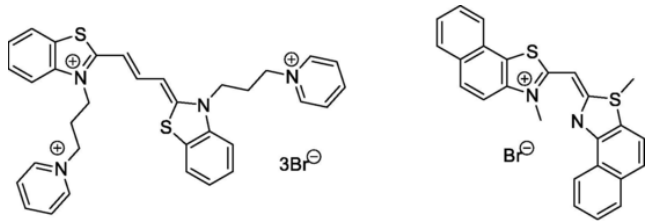

PP65 PP66

Fig. 35. Chemical structures of **PP65** and **PP66**.

taining push–pull dyes is waster waste treatment and environmental remediation. Indeed, photodegradation of pollutants is a hot research topic requiring the use of photocatalysts to proceed [239-244]. In this field, the use of three-component photoinitiating systems render the photopolymerization process photocatalytic so that the dyes used as the photosensitizers to initiate the polymerization process could be latter used for the photodegradation of pollutants. In this field, an interesting example has been recently published with a polyoxometalate used as the photocatalyst for photopolymerization and as the photocatalyst for the photodegradation of Eosin-Y [245,246]. Interest of this strategy relies on the possibility to regenerate the photocatalyst after use, by simply immersing the polymer composites into a diluted solution of hydrogen peroxide. If the proof of concept has been established with inorganic structures, this approach could be extended to push–pull dyes.

3. Conclusions

In this review, 68 push–pull dyes differing by the electron donors and the electron-acceptors have been presented and discussed. From an absorption viewpoint, push–pull dyes are appealing candidates by the facile tunability of their absorption spectra (See Fig. 38). Push-pull dyes are also exciting candidates from a synthetic viewpoint considering that their synthesis mostly based on Knoevenagel condensations which can be carried out in environmentally friendly conditions, in ethanol while using a catalytic amount of base. Parallel to this, the workup following the synthesis is often reduced to a simple filtration, facilitating the purification. Especially, filtration is a procedure which is easy to handle in industry.

However, irregular photoinitiating abilities have often been detected with these chromophores, which cannot simply be explained by their excited state lifetimes, their molar extinction coefficients or their redox properties. Indeed, a few works have clearly evidenced the relationship existing between the solvatochromic behavior and the polymerization efficiency. Considering that dyes that are not capable to give linear correlations using the Lippert-Mataga's, Bakhshiev's, Kawski-Chamma-Viallet's, McRae's and Suppan's polarity scales are also unable to initiate a polymerization process, examination of the solvatochromism can be even considered as a practical tool to anticipate the ability or not of a push–pull dye for photoinitiation. This review has also pinpointed that a few dyes such as **PP13**, **PP44** and **PP45** were capable to provide after photopolymerization colorless coatings, what is highly researched by industry. Indeed, the strong color imposed by the visible light photoinitiators is often considered as a major drawback of the visible light photopolymerization. By interrupting the electronic delocalization between the donor and the acceptor in the push–pull dye, an efficient discoloration can be obtained.

Future prospects will certainly consist in finding new tools to better anticipate the photoreactivity of the D-π-A-type push–pull dyes which remains from a synthetic viewpoint the most interesting light-absorbing materials for photoinitiation.

Uncited reference

[246].

Declaration of Competing Interest

The authors declare that they have no known competing financial interests or personal relationships that could have appeared to influence the work reported in this paper.

Acknowledgements

The authors thank Aix Marseille University and The Centre National de la Recherche (CNRS) for financial supports. The Agence Nationale de la Recherche (ANR agency) is acknowledged for its financial support through the PhD grants of Corentin Pigot (ANR-17-CE08-0010 DUALITY project) and Guillaume Noirbent (ANR-17-CE08-0054 VISICAT project). The Direction Générale de l'Armement (DGA)/Agence Innovation Defense (AID) is acknowledged for its financial support through the PhD grant of Damien Brunel.

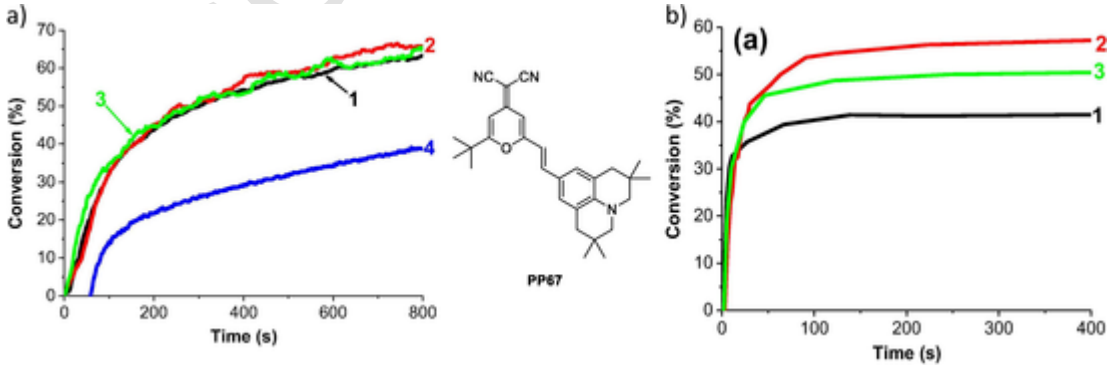

Fig. 36. a) Photopolymerization profiles of EPOX under air (1) **PP67**/Iod (0.5%/2%, w/w), (2) **PP67**/Iod/NVK (0.5%/2%/3%, w/w/w) with an halogen lamp, **PP67**/Iod/NVK (0.5%/2%/3%, w/w/w) upon with a laser diode at 532 nm (3) or 473 nm (4); b) Photopolymerization profiles of TMPTA in laminate for (1) **PP67**/Iod/NVK (0.5%/2%/3%, w/w/w), (2) **PP67**/MDEA/R'-Cl (0.5%/2%/1%, w/w/w) upon irradiation with an halogen lamp; (3) **PP67**/MDEA/R'-Cl (0.5%/2%/1%, w/w/w) upon irradiation with a laser diode at 532 nm. Reproduced with permission from Xiao et al. [231]. Copyright 2014 American Chemical Society.

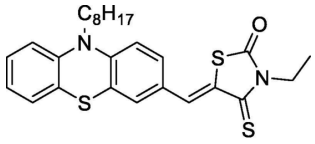

PP68

Fig. 37. Chemical structure of **PP68**.

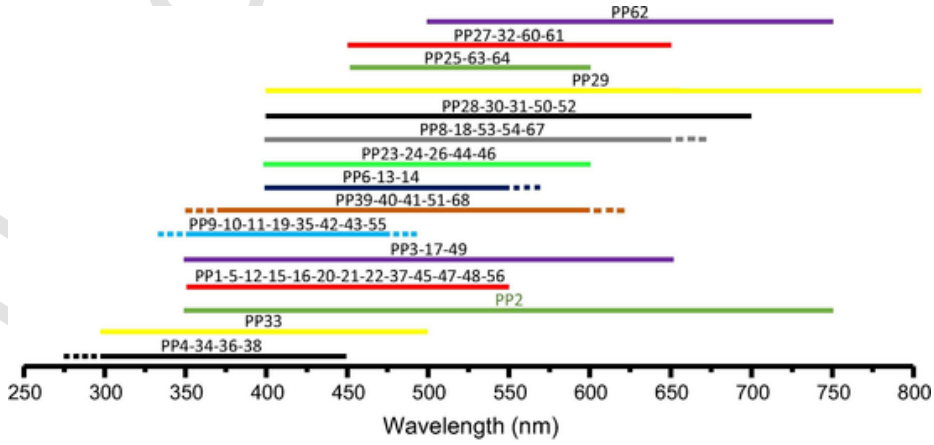

Fig. 38. Absorption range of the different dyes discussed in this review.

References

[1] P Xiao, J Zhang, F Dumur, M-A Tehfe, F Morlet-Savary, B Graff, D Gigmes, J-P Fouassier, J Lalevée, Visible light sensitive photoinitiating systems: Recent progress in cationic and radical photopolymerization reactions under soft conditions, Prog. Polym. Sci. 41 (2015) 32–66.

[2] C Mendes-Felipe, J Oliveira, I Etxebarria, J L Vilas-Vilela, S Lanceros-Mendez, State-of-the-art and future challenges of UV curable polymer-based smart materials for printing technologies, Adv. Mater. Technol. 4 (2019) 1800618.

[3] V Shukla, M Bajpai, D K Singh, M Singh, R Shukla, Review of basic chemistry of UV-curing technology, Pigm. Resin Technol. 33 (2004) 272–279.

[4] M Chen, M Zhong, J A Johnson, Light-controlled radical polymerization: mechanisms, methods, and applications, Chem. Rev. 116 (2016) 10167–10211.

[5] J V Crivello, E Reichmanis, Photopolymer materials and processes for advanced technologies, Chem. Mater. 26 (2014) 533–548.

[6] S Genty, P Tingaut, M Aufray, Fast polymerization at low temperature of an infrared radiation cured epoxy-amine adhesive, Thermochim Acta 666 (2018) 27–35.

[7] Z Zhang, N Corrigan, A Bagheri, J Jin, C Boyer, A versatile 3D and 4D printing system through photocontrolled raft polymerization, Angew. Chem. 131 (2019) 18122–18131.

[8] A Y Lee, J An, C K Chua, Two-way 4D-printing: a review on the reversibility of 3d-printed shape memory materials, Engineering 3 (2017) 663–674.

[9] A Bagheri, J Jin, Photopolymerization in 3D Printing, ACS Appl. Polym. Mater. 1 (2019) 593–611.

[10] D C Aduba Jr., E D Margaretta, A E C Marnot, K V Heifferon, W R Surbey, N A Chartrain, A R Whittington, T E Long, C B Williams, Vat photopolymerization 3D printing of acid-cleavable PEG-methacrylate networks for biomaterial applications, Mater. Today Commun. 19 (2019) 204–211.

[11] C Dietlin, S Schweizer, P Xiao, J Zhang, F Morlet-Savary, B Graff, J-P Fouassier, J Lalevée, Photopolymerization upon LEDs: new photoinitiating systems and strategies, Polym. Chem. 6 (2015) 3895–3912.

[12] J-P Fouassier, X Allonas, D Burget, Photopolymerization reactions under visible lights: principle, mechanisms and examples of applications, Prog. Org. Coat. 47 (2003) 16–36.

[13] J-T Lin, D-C Cheng, K-T Chen, H-W Liu, Dual-wavelength (UV and blue) controlled photopolymerization confinement for 3D-printing: Modeling and analysis of measurements, Polymers 11 (2019) 1819.

[14] J Lalevée, H Mokbel, J-P Fouassier, Recent developments of versatile photoinitiating systems for cationic ring opening polymerization operating at any wavelengths and und.er low light intensity sources, Molecules 20 (2015) 7201–7221.

[15] M-A Tehfe, F Louradour, J Lalevée, J-P Fouassier, Photopolymerization reactions: on the way to a green and sustainable chemistry, Appl. Sci. 3 (2013) 490–514.

[16] L K Kostanski, Y-M Kim, J F Macgregor, A E Hamielec, Cationic polymerization using mixed cationic photoinitiator systems, Des. Monomers Polym. 10 (2007) 327–345.

[17] A H Bonardi, F Dumur, T M Grant, G Noirbent, D Gigmes, B H Lessard, J-P Fouassier, J Lalevée, High performance near infrared (NIR) photoinitiating systems operating under low light intensity and in presence of oxygen, Macromolecules 51 (2018) 1314–1324.

[18] M Abdallah, H Le, A Hijazi, B Graff, F Dumur, T-T Bui, F Goubard, J-P Fouassier, J Lalevée, Acridone derivatives as high performance visible light photoinitiators for cationic and radical photosensitive resins for 3D printing technology and for low migration photopolymer property, Polymer 159 (2018) 47–58.

[19] J Zhang, F Dumur, M Bouzrati, P Xiao, C Dietlin, F Morlet-Savary, B Graff, D Gigmes, J-P Fouassier, J Lalevée, Novel panchromatic photo-polymerizable matrices: N, N'-dibutyl-quinacridone as an efficient and versatile photoinitiator, J. Polym. Sci. A Polym. Chem. 53 (2015) 1719–1727.

[20] M-A Tehfe, F Dumur, E Contal, B Graff, D Gigmes, J-P Fouassier, J Lalevée, Novel highly efficient organophotocatalysts: truxene-acridine-1,8-diones as photoinitiators of polymerization, Macromol. Chem. Phys. 214 (2013) 2189–2201.

[21] P Xiao, F Dumur, M-A Tehfe, B Graff, D Gigmes, J-P Fouassier, J Lalevée, Acridinediones: effect of substituents on their photoinitiating abilities in radical and cationic photopolymerization, Macromol. Chem. Phys. 214 (2013) 2276–2282.

[22] M-A Tehfe, F Dumur, B Graff, F Morlet-Savary, D Gigmes, J-P Fouassier, J Lalevée, Design of new Type I & Type II photoinitiators possessing highly coupled pyrene-ketone moieties, Polym. Chem. 4 (2013) 2313–2324.

[23] P Xiao, F Dumur, B Graff, D Gigmes, J-P Fouassier, J Lalevée, Variations on the benzophenone skeleton: novel high-performance blue light sensitive photoinitiating systems, Macromolecules 46 (2013) 7661–7667.

[24] J Zhang, M Frigoli, F Dumur, P Xiao, L Ronchi, B Graff, F Morlet-Savary, J-P Fouassier, D Gigmes, J Lalevée, Design of novel photoinitiators for radical and cationic photopolymerizations under Near UV and Visible LEDs (385, 395 and 405 nm), Macromolecules 47 (2014) 2811–2819.

[25] A Allushi, C Kutahya, C Aydogan, J Kreutzer, G Yilmaz, Y Yagci, Conventional Type II photoinitiators as activators for photoinduced metal-free atom transfer radical polymerization, Polym. Chem. 8 (2017) 1972–1977.

[26] E A Kamoun, A Winkel, M Eisenburger, H Menzel, Carboxylated camphorquinone as visible-light photoinitiator for biomedical application: Synthesis, characterization, and application, Arab. J. Chem. 9 (2016) 745–754.

[27] A Santini, I T Gallegos, C M Felix, Photoinitiators in dentistry: a review, Prim. Dent. J. 2 (2013) 30–33.

[28] J Zhang, D Campolo, F Dumur, P Xiao, D Gigmes, J-P Fouassier, J Lalevée, The carbazole-bound ferrocenium salt as a specific cationic photoinitiator upon near-UV and visible LEDs (365–405 nm), Polym. Bull. 73 (2016) 493–507.

[29] A Al Mousawi, F Dumur, J Toufaily, T Hamieh, B Graff, D Gigmes, J-P Fouassier, J Lalevée, Carbazole scaffold based photoinitiators/photoredox catalysts for new LED projector 3D printing resins, Macromolecules 50 (2017) 2747–2758.

[30] A Al Mousawi, D Magaldi Lara, G Noirbent, F Dumur, J Toufaily, T Hamieh, T-T Bui, F Goubard, B Graff, D Gigmes, J-P Fouassier, J Lalevée, Carbazole derivatives with thermally activated delayed fluorescence property as photoinitiators/ photoredox catalysts for LED 3D printing technology, Macromolecules 50 (2017) 4913–4926.

[31] A Al Mousawi, P Garra, F Dumur, T-T Bui, F Goubard, J Toufaily, T Hamieh, B Graff, D Gigmes, J-P Fouassier, J Lalevée, Novel carbazole skeleton-based photoinitiators for LED polymerization and LED projector 3D printing, Molecules 22 (2018) 2143.

[32] A Al Mousawi, A Arar, M Ibrahim-Ouali, S Duval, F Dumur, P Garra, J Toufaily, T Hamieh, B Graff, D Gigmes, J-P Fouassier, J Lalevée, Carbazole-based compounds as photoinitiators for free radical and cationic polymerization upon near visible light illumination, Photochem. Photobiol. Sci. 17 (2018) 578–585.

[33] M Abdallah, D Magaldi, A Hijazi, B Graff, F Dumur, J-P Fouassier, T-T Bui, F Goubard, J Lalevée, Development of new high performance visible light photoinitiators based on carbazole scaffold and their applications in 3D printing and photocomposite synthesis, J. Polym. Sci. A Polym. Chem. 57 (2019) 2081–2092.

[34] M-A Tehfe, F Dumur, P Xiao, M Delgove, B Graff, J-P Fouassier, D Gigmes, J Lalevée, Chalcone derivatives as highly versatile photoinitiators for radical, cationic, thiol-ene and IPN polymerization reactions upon visible lights, Polym. Chem. 5 (2014) 382–390.

[35] L Tang, J Nie, X Zhu, A high performance phenyl-free LED photoinitiator for cationic or hybrid photopolymerization and its application in LED cationic 3D printing, Polym. Chem. 11 (2020) 2855–2863.

[36] M-A Tehfe, F Dumur, P Xiao, B Graff, F Morlet-Savary, J-P Fouassier, D Gigmes, J Lalevée, New chromone based photoinitiators for polymerization reactions upon visible lights, Polym. Chem. 4 (2013) 4234–4244.

[37] A. Al Mousawi, P. Garra, M. Schmitt, J. Toufaily, T. Hamieh, B. Graff, J.-P. Fouassier, F. Dumur, J. Lalevée, 3-Hydroxyflavone and N-phenyl-glycine in high performance photoinitiating systems for 3D printing and photocomposites synthesis, Macromolecules 51 (2018) 4633-4641.

[38] J You, H Fu, D Zhao, T Hu, J Nie, T Wang, Flavonol dyes with different substituents in photopolymerization, J. Photochem. Photobiol. A: Chem. 386 (2020) 112097.

[39] M Abdallah, A Hijazi, B Graff, J-P Fouassier, G Rodeghiero, A Gualandi, F Dumur, P G Cozzi, J Lalevée, Coumarin derivatives as high performance visible light photoinitiators/photoredox catalysts for photosensitive resins for 3D printing technology, photopolymerization in water and photocomposites synthesis, Polym. Chem. 10 (2019) 872–884.

[40] Z Li, X Zou, G Zhu, X Liu, R Liu, Coumarin-based oxime esters: photobleachable and versatile unimolecular initiators for acrylate and thiol-based click photopolymerization under visible light-emitting diode light irradiation, ACS Appl. Mater. Interfaces 10 (2018) 16113–16123.

[41] M Abdallah, F Dumur, A Hijazi, G Rodeghiero, A Gualandi, P G Cozzi, J Lalevée, Keto-coumarin scaffold for photo-initiators for 3D printing and photo-composites, J. Polym. Sci. 58 (2020) 1115–1129.

[42] M Abdallah, A Hijazi, F Dumur, J Lalevée, Coumarins as powerful photosensitizers for the cationic polymerization of epoxy-silicones under near-UV and visible light and applications for 3D printing technology, Molecules 25 (2020) 2063.

[43] Q Chen, Q Yang, P Gao, B Chi, J Nie, Y He, Photopolymerization of coumarin-containing reversible photoresponsive materials based on wavelength selectivity, Ind. Eng. Chem. Res. 58 (2019) 2970–2975.

[44] P Xiao, F Dumur, J Zhang, J-P Fouassier, D Gigmes, J Lalevée, Copper complexes in radical photoinitiating systems: applications to free radical and cationic polymerization under visible lights, Macromolecules 47 (2014) 3837–3844.

[45] P Xiao, F Dumur, J Zhang, D Gigmes, J-P Fouassier, J Lalevée, Copper complexes: the effect of ligands on their photoinitiation efficiencies in radical polymerization reactions under visible light, Polym. Chem. 5 (2014) 6350–6357.

[46] P Xiao, J Zhang, D Campolo, F Dumur, D Gigmes, J-P Fouassier, J Lalevée, Copper and iron complexes as visible-light-sensitive photoinitiators of polymerization, J. Polym. Sci. A Polym. Chem. 53 (2015) 2673–2684.

[47] A Al Mousawi, A Kermagoret, D-L Versace, J Toufaily, T Hamieh, B Graff, F Dumur, D Gigmes, J-P Fouassier, J Lalevée, Copper photoredox catalysts for polymerization upon near UV or visible light: structure/reactivity/ efficiency relationships and use in LED projector 3D printing resins, Polym. Chem. 8 (2017) 568–580.

[48] P. Garra, A. Kermagoret, A. Al Mousawi, F. Dumur, D. Gigmes, F. Morlet-Savary, C. Dietlin, J.-P. Fouassier, J. Lalevée, New copper(I) complex based initiating systems in redox polymerization and comparison with the amine/benzoyl peroxide reference, Polym. Chem. 8 (2017) 4088-4097.

[49] P Garra, F Dumur, F Morlet-Savary, C Dietlin, D Gigmes, J-P Fouassier, J Lalevée, Mechanosynthesis of a copper complex for redox initiating systems with a unique near infrared light activation, J. Polym. Sci. A Polym. Chem. 55 (2017) 3646–3655.

[50] H Mokbel, D Anderson, R Plenderleith, C Dietlin, F Morlet-Savary, F Dumur, D Gigmes, J-P Fouassier, J Lalevée, Copper photoredox catalyst "G1": A new high

performance photoinitiator for near-UV and visible LEDs, Polym. Chem. 8 (2017) 5580–5592.
[51] P Garra, F Dumur, A Al Mousawi, B Graff, D Gigmes, F Morlet-Savary, C Dietlin, J-P Fouassier, J Lalevée, Mechanosynthesized Copper (I) complex based initiating systems for redox polymerization: towards upgraded oxidizing and reducing agents, Polym. Chem. 8 (2017) 5884–5896.
[52] P Garra, M Carré, F Dumur, F Morlet-Savary, C Dietlin, D Gigmes, J-P Fouassier, J Lalevée, Copper-based (photo) redox initiating systems as highly efficient systems for interpenetrating polymer network preparation, Macromolecules 51 (2018) 679–688.
[53] P Garra, F Dumur, M Nechab, F Morlet-Savary, C Dietlin, B Graff, D Gigmes, J-P Fouassier, J Lalevée, Stable copper acetylacetonate-based oxidizing agents in redox (NIR photoactivated) polymerization: an opportunity for one pot grafting from approach and example on a 3D printed object, Polym. Chem. 9 (2018) 2173–2182.
[54] H Mokbel, D Anderson, R Plenderleith, C Dietlin, F Morlet-Savary, F Dumur, D Gigmes, J-P Fouassier, J Lalevée, Simultaneous initiation of radical and cationic polymerization reactions using the "G1" copper complex as photoRedox catalyst: Applications of free radical/cationic hybrid photo-polymerization in the composites and 3D printing fields, Prog. Org. Coat. 132 (2019) 50–61.
[55] J Li, X Zhang, S Ali, M Y Akram, J Nie, X Zhu, The effect of polyethylene glycoldiacrylate complexation on type II photoinitiator and promotion for visible light initiation system, J. Photochem. Photobiol. A: Chem. 384 (2019) 112037.
[56] J Li, S Li, Y Li, R Li, J Nie, X Zhu, In situ monitoring of photopolymerization by photoinitiator with luminescence characteristics, J. Photochem. Photobiol. A: Chem. 389 (2020) 112225.
[57] J Li, Y Hao, M Zhong, L Tang, J Nie, X Zhu, Synthesis of furan derivative as LED light photoinitiator: one-pot, low usage, photobleaching for light color 3D printing, Dyes Pigm. 165 (2019) 467–473.
[58] J Zhang, J Lalevée, J Zhao, B Graff, M H Stenzel, P Xiao, Dihydroxyanthraquinone derivatives: natural dyes as blue-light-sensitive versatile photoinitiators of photopolymerization, Polym. Chem. 7 (2016) 7316–7324.
[59] P Xiao, F Dumur, D Thirion, S Fagour, S Vacher, X Sallenave, F Morlet-Savary, B Graff, J-P Fouassier, D Gigmes, J Lalevée, Multicolor photoinitiators for radical and cationic polymerization: mono vs. poly functional thiophene derivatives, Macromolecules 46 (2013) 6786–6793.
[60] J Zhang, N Zivic, F Dumur, C Guo, Y Li, P Xiao, B Graff, D Gigmes, J-P Fouassier, J Lalevée, Panchromatic photoinitiators for radical, cationic and thiol-ene polymerization reactions: a search in the diketopyrrolopyrrole or indigo dye series, Mater. Today Commun. 4 (2015) 101–108.
[61] P Xiao, W Hong, Y Li, F Dumur, B Graff, J-P Fouassier, D Gigmes, J Lalevée, Diketopyrrolopyrrole dyes: structure/reactivity/efficiency relationship in photoinitiating systems upon visible lights, Polymer 55 (2014) 746–751.
[62] P Xiao, W Hong, Y Li, F Dumur, B Graff, J-P Fouassier, D Gigmes, J Lalevée, Green light sensitive diketopyrrolopyrrole derivatives used in versatile photoinitiating systems for photopolymerizations, Polym. Chem. 5 (2014) 2293–2300.
[63] A Al Mousawi, P Garra, F Dumur, B Graff, J-P Fouassier, J Lalevée, Flavones as natural photoinitiators for light mediated free radical polymerization via light emitting diodes, J. Polym. Sci. A Polym. Chem. 58 (2020) 254–262.
[64] A. Al Mousawi, P. Garra, M. Schmitt, J. Toufaily, T. Hamieh, B. Graff, J.-P. Fouassier, F. Dumur, J. Lalevée, 3-Hydroxyflavone and N-phenyl-glycine in high performance photo-initiating systems for 3D printing and photocomposites synthesis, Macromolecules 51 (2018) 4633-4641.
[65] P Garra, D Brunel, G Noirbent, B Graff, F Morlet-Savary, C Dietlin, V F Sidorkin, F Dumur, D Duché, D Gigmes, J-P Fouassier, J Lalevée, Ferrocene-based (photo)redox polymerization under long wavelengths, Polym. Chem. 10 (2019) 1431–1441.
[66] H Mokbel, J Toufaily, T Hamieh, F Dumur, D Campolo, D Gigmes, J-P Fouassier, J Ortyl, J Lalevee, Specific cationic photoinitiators for Near UV and visible LEDs: Iodonium vs. ferrocenium structures, J. Appl. Polym. Sci. 132 (2015) 42759.
[67] A Al Mousawi, F Dumur, P Garra, J Toufaily, T Hamieh, F Goubard, T-T Bui, B Graff, D Gigmes, J-P Fouassier, J Lalevée, Azahelicenes as visible light photoinitiators for cationic and radical polymerization: preparation of photo-luminescent polymers and use in high performance LED projector 3D printing resins, J. Polym. Sci. A Polym. Chem. 55 (2017) 1189–1199.
[68] A Al Mousawi, M Schmitt, F Dumur, J Ouyang, L Favereaud, V Dorcet, N Vanthuyne, P Garra, J Toufaily, T Hamieh, B Graff, J-P Fouassier, D Gigmes, J Crassous, J Lalevée, Visible light chiral photoinitiator for radical polymerization and synthesis of polymeric films with strong chiroptical activity, Macromolecules 51 (2018) 5628–5637.
[69] S Villotte, D Gigmes, F Dumur, J Lalevée, Design of iodonium salts for UV or Near-UV LEDs for photoacid generator and polymerization purposes, Molecules 25 (2020) 149.
[70] N Zivic, M Bouzrati-Zerrelli, S Villotte, F Morlet-Savary, C Dietlin, F Dumur, D Gigmes, J-P Fouassier, J Lalevée, A novel naphthalimide scaffold based iodonium salt as a one-component photoacid/photoinitiator for cationic and radical polymerization under LED exposure, Polym. Chem. 7 (2016) 5873–5879.
[71] J Lalevée, M Peter, F Dumur, D Gigmes, N Blanchard, M-A Tehfe, F Morlet-Savary, J-P Fouassier, Subtle ligand effects in oxidative photocatalysis with iridium complexes: application to photopolymerization, Chem. Eur. J. 17 (2011) 15027–15031.
[72] J Lalevée, M-A Tehfe, F Dumur, D Gigmes, N Blanchard, F Morlet-Savary, J-P Fouassier, Iridium photocatalysts in free radical photopolymerization under visible lights, ACS Macro Lett. 1 (2012) 286–290.
[73] J Lalevée, F Dumur, C R Mayer, D Gigmes, G Nasr, M-A Tehfe, S Telitel, F Morlet-Savary, B Graff, J-P Fouassier, Photopolymerization of N-vinylcarbazole using visible-light harvesting iridium complexes as photoinitiators, Macromolecules 45 (2012) 4134–4141.
[74] S Telitel, F Dumur, S Telitel, O Soppera, M Lepeltier, Y Guillaneuf, J Poly, F Morlet-Savary, P Fioux, J-P Fouassier, D Gigmes, J Lalevée, Photoredox catalysis using a new iridium complex as an efficient toolbox for radical, cationic and controlled polymerizations under soft blue to green lights, Polym. Chem. 6 (2015) 613–624.
[75] S Telitel, F Dumur, M Lepeltier, D Gigmes, J-P Fouassier, J Lalevée, Photoredox process induced polymerization reactions: iridium complexes for panchromatic photo-initiating systems, C.R. Chimie 19 (2016) 71–78.
[76] M-A Tehfe, M Lepeltier, F Dumur, D Gigmes, J-P Fouassier, J Lalevée, Structural effects in the iridium complex series: photoredox catalysis and photoinitiation of polymerization reactions under visible lights, Macromol. Chem. Phys. 218 (2017) 1700192.
[77] J Zhang, D Campolo, F Dumur, P Xiao, J-P Fouassier, D Gigmes, J Lalevée, Iron complexes as photoinitiators for radical and cationic polymerization through photoredox catalysis processes, J. Polym. Sci. A Polym. Chem. 53 (2015) 42–49.
[78] S Telitel, F Dumur, D Campolo, J Poly, D Gigmes, J-P Fouassier, J Lalevée, Iron complexes as potential photocatalysts for controlled radical photopolymerizations: a tool for modifications and patterning of surfaces, J. Polym. Sci. A Polym. Chem. 54 (2016) 702–713.
[79] J Zhang, D Campolo, F Dumur, P Xiao, J-P Fouassier, D Gigmes, J Lalevée, Visible-light-sensitive photoredox catalysis by iron complexes: applications in cationic and radical polymerization reactions, J. Polym. Sci. A Polym. Chem. 54 (2016) 2247–2253.
[80] J Zhang, D Campolo, F Dumur, P Xiao, J-P Fouassier, D Gigmes, J Lalevée, Novel iron complexes in visible-light-sensitive photoredox catalysis: effect of ligands on their photoinitiation efficiencies, ChemCatChem 8 (2016) 2227–2233.
[81] J Zhang, F Dumur, P Horcajada, C Livage, P Xiao, J-P Fouassier, D Gigmes, J Lalevée, Iron-based metal-organic frameworks (MOF) as photocatalysts for radical and cationic polymerizations under near UV and visible LEDs (385–405 nm), Macromol. Chem. Phys. 217 (2016) 2534–2540.
[82] A-H Bonardi, S Zahouily, C Dietlin, B Graff, F Morlet-Savary, M Ibrahim-Ouali, D Gigmes, N Hoffmann, F Dumur, J Lalevée, New 1,8-naphthalimide derivatives as photoinitiators for free radical polymerization upon visible light, Catalysts 9 (2019) 637.
[83] J Zhang, N Zivic, F Dumur, P Xiao, B Graff, J-P Fouassier, D Gigmes, J Lalevée, Naphthalimide-tertiary amine derivatives as blue-light-sensitive photoinitiators, ChemPhotoChem 2 (2018) 481–489.
[84] P Xiao, F Dumur, J Zhang, B Graff, D Gigmes, J-P Fouassier, J Lalevée, Naphthalimide derivatives: substituent effects on the photoinitiating ability in polymerizations under near UV, purple, white and blue LEDs (385 nm, 395 nm, 405 nm, 455 nm or 470 nm), Macromol. Chem. Phys. 216 (2015) 1782–1790.
[85] P Xiao, F Dumur, J Zhang, B Graff, D Gigmes, J-P Fouassier, J Lalevée, Naphthalimide-phthalimide derivative based photoinitiating systems for polymerization reactions under blue lights, J. Polym. Sci. A Polym. Chem. 53 (2015) 665–674.
[86] J Zhang, N Zivic, F Dumur, P Xiao, B Graff, D Gigmes, J-P Fouassier, J Lalevée, A benzophenone-naphthalimide derivative as versatile photoinitiator for near UV and visible lights, J. Polym. Sci. A Polym. Chem. 53 (2015) 445–451.
[87] J Zhang, N Zivic, F Dumur, P Xiao, B Graff, J-P Fouassier, D Gigmes, J Lalevée, *N*-[2-(dimethylamino)ethyl]-1,8-naphthalimide derivatives as photoinitiators under LEDs, Polym. Chem. 9 (2018) 994–1003.
[88] N Zivic, J Zhang, D Bardelang, F Dumur, P Xiao, T Jet, D-L Versace, C Dietlin, F Morlet-Savary, B Graff, J-P Fouassier, D Gigmes, J Lalevée, Novel naphthalimideamine based photoinitiators operating under violet and blue LEDs and usable for various polymerization reactions and synthesis of hydrogels, Polym. Chem. 7 (2016) 418–429.
[89] J Zhang, F Dumur, P Xiao, B Graff, D Bardelang, D Gigmes, J-P Fouassier, J Lalevée, Structure design of naphthalimide derivatives: towards versatile photo-initiators for near UV/Visible LEDs, 3D printing and water soluble photoinitiating systems, Macromolecules 48 (2015) 2054–2063.
[90] J Zhang, N Zivic, F Dumur, P Xiao, B Graff, J-P Fouassier, D Gigmes, J Lalevée, UV violet-blue LED induced polymerizations: specific photoinitiating systems at 365, 385, 395 and 405 nm, Polymer 55 (2014) 6641–6648.
[91] P Xiao, F Dumur, B Graff, D Gigmes, J-P Fouassier, J Lalevée, Blue light sensitive dyes for various photopolymerization reactions: naphthalimide and naphthalic anhydride derivatives, Macromolecules 47 (2014) 601–608.
[92] P Xiao, F Dumur, M Frigoli, M-A Tehfe, B Graff, J-P Fouassier, D Gigmes, J Lalevée, Naphthalimide based methacrylated photoinitiators in radical and cationic photopolymerization under visible light, Polym. Chem. 4 (2013) 5440–5448.
[93] G Noirbent, F Dumur, Recent advances on naphthalic anhydrides and 1,8-naphthalimide-based photoinitiators of polymerization, Eur. Polym. J. (2020), doi:10.1016/j.eurpolymj.2020.109702.
[94] P Xiao, F Dumur, M Frigoli, B Graff, F Morlet-Savary, G Wantz, H Bock, J-P Fouassier, D Gigmes, J Lalevée, Perylene derivatives as photoinitiators in blue light sensitive cationic or radical curable films and panchromatic thiol-ene polymerizable films, Eur. Polym. J. 53 (2014) 215–222.
[95] M-A Tehfe, F Dumur, B Graff, D Gigmes, J-P Fouassier, J Lalevée, Green light induced cationic ring opening polymerization reactions: perylene-3,4:9,10-*bis*(dicarboximide) as efficient photosensitizers, Macromol. Chem. Phys. 214 (2013) 1052–1060.

[96] P Xiao, F Dumur, B Graff, D Gigmes, J-P Fouassier, J Lalevée, Red-light-induced cationic photopolymerization: perylene derivatives as efficient photoinitiators, Macromol. Rapid Commun. 34 (2013) 1452–1458.
[97] M Abdallah, T-T Bui, F Goubard, D Theodosopoulou, F Dumur, A Hijazi, J-P Fouassier, J Lalevée, Phenothiazine derivatives as photoredox catalysts for cationic and radical photosensitive resins for 3D printing technology and photocomposites synthesis, Polym. Chem. 10 (2019) 6145–6156.
[98] A Bonardi, F Bonardi, G Noirbent, F Dumur, C Dietlin, D Gigmes, J-P Fouassier, J Lalevée, Different NIR dye scaffolds for polymerization reactions under NIR light, Polym. Chem. 10 (2019) 6505–6514.
[99] A Al Mousawi, C Poriel, F Dumur, J Toufaily, T Hamieh, J-P Fouassier, J Lalevée, Zinc-tetraphenylporphyrin as high performance visible-light photoinitiator of cationic photosensitive resins for LED projector 3D printing applications, Macromolecules 50 (2017) 746–753.
[100] M-A Tehfe, F Dumur, B Graff, F Morlet-Savary, D Gigmes, J-P Fouassier, J Lalevée, Design of new Type I and Type II photoinitiators possessing highly coupled pyrene-ketone moieties, Polym. Chem. 4 (2013) 2313–2324.
[101] M-A Tehfe, F Dumur, E Contal, B Graff, D Gigmes, F Morlet-Savary, J-P Fouassier, J Lalevée, New insights in radical and cationic polymerizations upon visible light exposure: role of novel photoinitiator systems based on the pyrene chromophore, Polym. Chem. 4 (2013) 1625–1634.
[102] S Telitel, F Dumur, T Faury, B Graff, M-A Tehfe, D Gigmes, J-P Fouassier, J Lalevée, New core-pyrene π-structure organophotocatalysts usable as highly efficient photoinitiators, Beilstein J. Org. Chem. 9 (2013) 877–890.
[103] F Dumur, Recent advances on pyrene-based photoinitiators of polymerization, Eur. Polym. J. 126 (2020) 109564.
[104] N Uchida, H Nakano, T Igarashi, T Sakurai, nonsalt 1-(arylmethyloxy)pyrene photoinitiators capable of initiating cationic polymerization, J. Appl. Polym. Sci. 131 (2014) 40510.
[105] A Mishra, S Daswal, 1-(Bromoacetyl)pyrene, a novel photoinitiator for the copolymerization of styrene and methylmethacrylate, Rad. Phys. Chem. 75 (2006) 1093–1100.
[106] N Karaca, N Ocala, N Arsua, S Jockusch, Thioxanthone-benzothiophenes as photoinitiator for free radical polymerization, J. Photochem. Photobiol. A: Chem. 331 (2016) 22–28.
[107] Q Wu, X Wang, Y Xiong, J Yang, H Tang, Thioxanthone based one-component polymerizable visible light photoinitiator for free radical polymerization, RSC Adv. 6 (2016) 66098–66107.
[108] J Qiu, J Wei, Thioxanthone photoinitiator containing polymerizable N-aromatic maleimide for photopolymerization, J. Polym. Res. 21 (2014) 559.
[109] S Dadashi-Silab, C Aydogan, Y Yagci, Shining a light on an adaptable photoinitiator: advances in photopolymerizations initiated by thioxanthones, Polym. Chem. 6 (2015) 6595–6615.
[110] W Jivaramonaikul, P Rashatasakhonc, S Wanichwecharungruang, UVA absorption and photostability of coumarins, Photochem. Photobiol. Sci. 9 (2010) 1120–1125.
[111] J Donovalová, M Cigáň, H Stankovičová, J Gašpar, M Danko, A Gáplovský, P Hrdlovič, Spectral properties of substituted coumarins in solution and polymer matrices, Molecules 17 (2012) 3259–3276.
[112] L Cisse, A Djande, M Capo-Chichi, A Khonté, J-P Bakhoum, F Delattre, J Yoda, A Saba, A Tine, J-J Aaron, Quantitative study of the substituent effects on the electronic absorption and fluorescence spectra of coumarins, J. Phys. Org. Chem. 33 (2020) e4014.
[113] H Wang, T E Kaiser, S Uemura, F Würthner, Perylene bisimide J-aggregates with absorption maxima in the NIR, Chem. Commun. 10 (2008) 1181–1183.
[114] S L Oliveira, D S Corrêa, L Misoguti, C J L Constantino, R F Aroca, S C Zilio, C R Mendonça, Perylene derivatives with large two-photon-absorption cross-sections for application in optical limiting and upconversion lasing, Adv. Mater. 17 (2005) 1890–1893.
[115] G A Kumar, J Thomas, N V Unnikrishnan, V P N Nampoori, C P G Vallabhan, Optical absorption and emission spectral studies of phthalocyanine molecules in DMF, J. Porphyr. Phthalocya. 5 (2001) 456–459.
[116] A A M Farag, Optical absorption studies of copper phthalocyanine thin films, Opt. Laser Technol. 39 (2007) 728–732.
[117] T Furuyama, K Satoh, T Kushiya, N Kobayashi, Design, synthesis, and properties of phthalocyanine complexes with main-group elements showing main absorption and fluorescence beyond 1000 nm, J. Am. Chem. Soc. 136 (2014) 765–776.
[118] K J Hamam, M I Alomari, A study of the optical band gap of zinc phthalocyanine nanoparticles using UV–Vis spectroscopy and DFT function, Appl. Nanosci. 7 (2017) 261–268.
[119] F Bureš, Fundamental aspects of property tuning in push–pull molecules, RSC Adv. 4 (2014) 58826–58851.
[120] J Podlesný, O Pytela, M Klikar, V Jelínková, I V Kityk, K Ozga, J Jedryka, M Rudysh, F Bureš, Small isomeric push–pull chromophores basedon thienothiophenes with tunable optical (non) linearities, Org. Biomol. Chem. 17 (2019) 3623–3634.
[121] A K Narsaria, J Poater, C Fonseca Guerra, A W Ehlers, T A Hamlin, K Lammertsma, M Bickelhaupt, Distortion-controlled redshift of organic dye molecules, Chem. Eur. J. 26 (2020) 2080–2093.
[122] S Pascal, Y A Getmanenko, Y Zhang, I Davydenko, M H Ngo, G Pilet, S Redon, Y Bretonnière, O Maury, I Ledoux-Rak, S Barlow, S R Marder, C Andraud, Design of near-infrared-absorbing unsymmetrical polymethinedyes with large quadratic hyperpolarizabilities, Chem. Mater. 30 (2018) 3410–3418.
[123] J Kulhaneka, F Bures, O Pytela, T Mikysek, J Ludvıkc, A Ruzicka, Push-pull molecules with a systematically extended p-conjugated system featuring 4,5-dicyanoimidazole, Dyes Pigm. 85 (2010) 57–65.
[124] M Klikar, K Seintis, I Polyzos, O Pytela, T Mikysek, N Almonasy, M Fakis, F Bureš, Star-shaped push-pull molecules with a varied number of peripheral acceptors: an insight into their optoelectronic features, ChemPhotoChem 2 (2018) 465–474.
[125] A Guerlin, F Dumur, E Dumas, F Miomandre, G Wantz, C R Mayer, Tunable optical properties of chromophores derived from oligo(*p*-phenylene vinylene), Org. Lett. 12 (2010) 2382–2385.
[126] C Pigot, G Noirbent, T-T Bui, S Péralta, D Gigmes, M Nechab, F Dumur, Push-pull chromophores based on the naphthalene scaffold: Potential candidates for optoelectronic applications, Materials 12 (2019) 1342.
[127] C Pigot, G Noirbent, S Peralta, S Duval, M Nechab, D Gigmes, F Dumur, Unprecedented nucleophilic attack of piperidine on the electron acceptor during the synthesis of push-pull dyes by a Knoevenagel reaction, Helv. Chim. Acta 102 (2019) e1900229.
[128] M-A Tehfe, F Dumur, B Graff, F Morlet-Savary, D Gigmes, J-P Fouassier, J Lalevée, Push–pull (thio)barbituric acid derivatives in dye photosensitized radical and cationic polymerization reactions under 457/473 nm laser beams or blue LEDs, Polym. Chem. 4 (2013) 3866–3875.
[129] M Klikar, V Jelínková, Z Růžičková, T Mikysek, O Pytela, M Ludwig, F Bureš, Malonic acid derivatives on duty as electron-withdrawing units in push–pull molecules, Eur. J. Org. Chem. 2764–2779 (2017).
[130] F Dumur, C R Mayer, E Dumas, F Miomandre, M Frigoli, F Sécheresse, New chelating stilbazonium-like dyes from Michler's ketone, Org. Lett. 10 (2008) 321–324.
[131] T A Khattab, H E Gaffer, Synthesis and application of novel tricyanofuran hydrazone dyes as sensors for detection of microbes, Color. Technol. 132 (2016) 460–465.
[132] M C Davis, T J Groshens, D A Parrish, Preparation of cyan dyes from 6-diethylaminobenzo[b]furan-2-carboxaldehyde, Synth. Commun. 1 (2010) 3008–3020.
[133] R Andreu, L Carrasquer, S Franco, J Garın, J Orduna, N M de Baroja, R Alicante, B Villacampa, M Allain, 4H-Pyran-4-ylidenes: Strong proaromatic donors for organic nonlinear optical chromophores, J. Org. Chem. 74 (2009) 6647–6657.
[134] R Andreu, E Galan, J Garin, V Herrero, E Lacarra, J Orduna, R Alicante, B Villacampa, Linear and v-shaped nonlinear optical chromophores with multiple 4H-pyran-4-ylidene moieties, J. Org. Chem. 75 (2010) 1684–1692.
[135] B R Cho, K H Son, S H Lee, Y S Song, Y K Lee, S J Jeon, J H Choi, H Lee, M Cho, Two photon absorption properties of 1,3,5-tricyano-2,4,6-tris(styryl)benzene derivatives, J. Am. Chem. Soc. 123 (2001) 10039–10045.
[136] X H Zhang, Y-H Zhan, D Chen, F Wang, L-Y Wang, Merocyanine dyes containing an isoxazolone nucleus: Synthesis, X-ray crystal structures, spectroscopic properties and DFT studies, Dyes Pigm. 93 (2012) 1408–1415.
[137] T Marinado, D P Hagberg, M Hedlund, T Edvinsson, E M J Johansson, G Boschloo, H Rensmo, T Brinck, L Sun, A Hagfeldty, Rhodanine dyes for dye-sensitized solar cells: spectroscopy, energy levels and photovoltaic performance, PCCP 11 (2009) 133–141.
[138] R Hirosawa, Y Akune, N Endo, S Hatano, T Hosokai, H Sato, A Matsumoto, A variety of solid-state fluorescence properties of pyrazine dyes depending on terminal substituents, Dyes Pigm. 146 (2017) 576–581.
[139] J Kulhanek, F Bures, A Wojciechowski, M Makowska-Janusik, E Gondek, I V Kityk, Optical operation by chromophores featuring 4,5-dicyanoimidazole embedded within poly(methyl methacrylate) matrices, J. Phys. Chem. A 114 (2010) 9440–9446.
[140] Z Ci, X Yu, M Bao, C Wang, T Ma, Influence of the benzo[d]thiazole-derived π-bridges on the optical and photovoltaic performance of D–π–A dyes, Dyes Pigm. 96 (2013) 619–625.
[141] G B Bodedla, K R Justin Thomas, M S Fan, K C Ho, Bi-anchoring organic dyes that contain benzimidazole branches for dye-sensitized solar cells: Effects of π spacer and peripheral donor groups, Chem. Asian J. 11 (2016) 2564–2577.
[142] A Baheti, K R Justin Thomas, C-P Lee, C-T Li, K-C Ho, Organic dyes containing fluoren-9-ylidene chromophores for efficient dye-sensitized solar cells, J. Mater. Chem. A 2 (2014) 5766–5779.
[143] G Noirbent, F Dumur, Recent advances on nitrofluorene derivatives: Versatile electron acceptors to create dyes absorbing from the visible to the near and far infrared region, Materials 11 (2018) 2425.
[144] E Knoevenagel, Ueber eine darstellungsweise des benzylidenacetessigesters, Ber. Dtsch. Chem. Ges. 29 (1896) 172–174.
[145] H. Li, T. Ming Koh, A. Hagfeldt, M. Grätzel, S.G. Mhaisalkar, A.C. Grimsdale, New donor–π–acceptor sensitizers containing 5H-[1, 2, 5] thiadiazolo [3, 4-f] isoindole-5, 7 (6H)-dione and 6 H-pyrrolo [3, 4-g] quinoxaline-6, 8 (7 H)-dione units, Chem. Commun. 49 (2013) 2409-2411.
[146] Y Oyama, Y Shimada, S Inoue, T Nagano, Y Fujikawa, K Komaguchi, I Imae, Y Harima, New molecular design of donor-π-acceptor dyes for dye-sensitized solar cells: control of molecular orientation and arrangement on TiO_2 surface, New J. Chem. 35 (2011) 111–118.
[147] J. Peet, J.Y. Kim, N.E. Coates, W.L. Ma, D. Moses, A.J. Heeger, G.C. Bazan, Efficiency enhancement in low-bandgap polymer solar cells by processing with alkane dithiols, Nat. Mater. 6 (2007) 497-500.
[148] G S He, L S Tan, Q Zheng, P N Prasad, Multiphoton absorbing materials: molecular designs, characterizations, and applications, Chem. Rev. 108 (2008) 1245–1330.
[149] F Dumur, D Gigmes, J-P Fouassier, J Lalevée, Organic Electronics: an El Dorado in the quest of new photoCatalysts as photoinitiators of polymerization, Acc. Chem. Res. 49 (2016) 1980–1989.
[150] M-A Tehfe, F Dumur, B Graff, D Gigmes, J-P Fouassier, J Lalevée, Blue-to-red light sensitive push−pull structured photoinitiators: indanedione derivatives for radical

and cationic photopolymerization reactions, Macromolecules 46 (2013) 3332–3341.
[151] F Dumur, C R Mayer, K Hoang-Thi, I Ledoux-Rak, F Miomandre, G Clavier, E Dumas, R Méallet-Renault, M Frigoli, J Zyss, F Sécheresse, Electrochemical, linear optical, and nonlinear optical properties and interpretation by Density Functional Theory calculations of (4-*N,* N-dimethylaminostyryl)pyridinium pendant group associated with polypyridinic ligands and respective multifunctional metal complexes ($R^{ul}I$ or $Z^{nl}I$), Inorg. Chem. 48 (2009) 8120–8133.
[152] C Reichardt, Solvatochromic dyes as solvent polarity indicators, Chem. Rev. 94 (1994) 2319–2358.
[153] M J Kamlet, J-L M Abboud, M H Abraham, R W Taft, Linear solvation energy relationships. 23. A comprehensive collection of the solvatochromic parameters,pi.*,alpha., and.beta., and some methods for simplifying the generalized solvatochromic equation, J. Org. Chem. 48 (1983) 2877–2887.
[154] J Catalan, On the ET (30), π*, Py, S‘, and SPP empirical scales as descriptors of nonspecific solvent effects, J. Org. Chem. 62 (1997) 8231–8234.
[155] E Lippert, Dipolmoment und elektronenstruktur von angeregten molekülen, Z. Naturforsch. 10a (1955) 541–545.
[156] N G Bakshiev, Universal intermolecular interactions and their effect on the position of the electronic spectra of molecules in two-component solutions. VII. Theory (general case of an isotropic solution), Opt Spektrosk. 16 (1964) 446.
[157] A Kawski, Der wellenzahl von elecktronenbanden lumineszie- renden molecule, Acta Phys. Polon. 29 (1966) 507–518.
[158] E G McRae, Theory of solvent effects on molecular electronic spectra. Frequency shifts, J. Phys. Chem. 61 (1957) 562–572.
[159] P Suppan, Solvent effects on the energy of electronic transitions: experimental observations and applications to structural problems of excited molecules, J. Chem. Soc. A 3125–3133 (1968).
[160] F Terenziani, A Painelli, C Katan, M Charlot, M Blanchard-Desce, Charge instability in quadrupolar chromophores: symmetry breaking and solvatochromism, J. Am. Chem. Soc. 128 (2006) 15742–15755.
[161] M S Najare, M K Patil, A A A Nadaf, S Mantur, M Garbhagudi, S Gaonkar, S R Inamdar, I A M Khazi, J. Mol. Struct. 1199 (2020) 127032.
[162] B Maity, A Chatterjee, D Seth, Photophysics of a coumarin in different solvents: use of different solvatochromic models, Photochem. Photobiol. 90 (2014) 734–746.
[163] S Dadashi-Silab, S Doran, Y Yagci, Photoinduced electron transfer reactions for macromolecular syntheses, Chem. Rev. 116 (2016) 10212–10275.
[164] J Xu, S Shanmugam, H T Duong, C Boyer, Organo-photocatalysts for photoinduced electron transfer-reversible addition–fragmentation chain transfer (PET-RAFT) polymerization, Polym. Chem. 6 (2015) 5615–5624.
[165] D Wang, P Garra, J-P Fouassier, B Graff, Y Yagci, J Lalevée, Indole-based charge transfer complexes as versatile dual thermal and photochemical polymerization initiators for 3D printing and composites, Polym. Chem. 10 (2019) 4991–5000.
[166] P Garra, B Graff, F Morlet-Savary, C Dietlin, J-M Becht, J-P Fouassier, J Lalevée, Charge transfer complexes as pan-scaled photoinitiating systems: from 50μm 3d printed polymers at 405 nm to extremely deep photopolymerization (31 cm), Macromolecules 51 (2018) 57–70.
[167] P. Tordo, Spin-trapping: recent developments and applications; N.M. Atherton, M.J. Davies, B.C. Gilbert, Eds.; Electron Spin Resonance 16; The Royal Society of Chemistry: Cambridge, U.K., 1998.
[168] L. Bornstein: Magnetic Properties of Free Radicals; H. Fischer, Ed.; Springer Verlag: Berlin, 2005; Vol. 26d.
[169] H Chandra, I M T Davidson, M C R Symons, Use of spin traps in the study of silyl radicals in the gas phase, J. Chem. Soc., Faraday Trans. 1 (79) (1983) 2705–2711.
[170] A Alberti, R Leardini, G F Pedulli, A Tundo, G Zanardi, Spin trapping of radicals centered at elements of groups, Gazz. Chim. Ital. 113 (1983) 869–871.
[171] Y Hua, J V Crivello, Synergistic interaction of epoxides and N-vinylcarbazole during photoinitiated cationic polymerization, J. Polym. Sci. A: Polym. Chem. 38 (2000) 3697–3709.
[172] Mohamad-Ali Tehfe, Frédéric Dumur, Bernadette Graff, Fabrice Morlet-Savary, Jean-Pierre Fouassier, Didier Gigmes, Jacques Lalevée, New push–pull dyes derived from michler's ketone for polymerization reactions upon visible lights, Macromolecules 46 (10) (2013) 3761–3770, doi:10.1021/ma400766z.
[173] P Xiao, F Dumur, B Graff, F Morlet-Savary, L Vidal, D Gigmes, J-P Fouassier, J Lalevée, Structural effects in the indanedione skeleton for the design of low intensity 300–500 nm light sensitive initiators, Macromolecules 47 (2014) 26–34.
[174] P Xiao, F Dumur, J Zhang, B Graff, D Gigmes, J-P Fouassier, J Lalevée, New role of aminothiazo-naphthalimide derivatives: outstanding photoinitiators for cationic and radical photopolymerizations under visible LEDs, RSC Adv. 6 (2016) 48684–48693.
[175] K. Sun, C. Pigot, H. Chen, M. Nechab, D. Gigmes, F. Morlet-Savary, B. Graff, S. Liu, P. Xiao, F. Dumur, J. Lalevée, Free radical photopolymerization and 3d printing using newly developed dyes: indane-1,3-dione and 1H-cyclopentanaphthalene-1,3-dione derivatives as photoinitiators in three-component systems, Catalysts 10 (2020) 463.
[176] C Pigot, G Noirbent, S Peralta, S Duval, T-T Bui, P-H Aubert, M Nechab, D Gigmes, F Dumur, New push-pull dyes based on 2-(3-oxo-2,3-dihydro-1*H*-cyclopenta[*b*]naph-thalen-1-ylidene)malononitrile: An amine-directed synthesis, Dyes Pigm. 175 (2020) 108182.
[177] B Steyrer, P Neubauer, R Liska, J Stampfl, Visible light photoinitiator for 3d-printing of tough methacrylate resins, Materials 10 (2017) 1445.
[178] H Quan, T Zhang, H Xu, S Luo, J Nie, X Zhu, Photo-curing 3D printing technique and its challenges, Bioact. Mater. 5 (2020) 110–115.
[179] H Lai, D Zhu, P Xiao, Yellow triazine as an efficient photoinitiator for polymerization and 3D printing under LEDs, Macromol. Chem. Phys. 220 (2019) 1900315.
[180] R Nazir, B Thorsted, E Balciunas, L Mazur, I Deperasinska, M Samoc, J Brewer, M Farsari, D T Gryko, π-Expanded 1,3-diketones – synthesis, optical properties and application in two-photon polymerization, J. Mater. Chem. C 4 (2016) 167–177.
[181] D Perevoznik, R Nazir, R Kiyan, K Kurselis, B Koszarna, D T Gryko, B N Chichkov, High-speed two-photon polymerization 3D printing with a microchip laser at its fundamental wavelength, Opt. Exp. 27 (2019) 25119.
[182] H Mokbel, F Dumur, S Telitel, L Vidal, P Xiao, D-L Versace, M-A Tehfe, F Morlet-Savary, B Graff, J-P Fouassier, D Gigmes, J Toufaily, T Hamieh, J Lalevée, Photoinitiating systems of polymerization and in situ incorporation of metal nanoparticles into polymer matrices upon exposure to visible light: push–pull malonate and malononitrile based dyes, Polym. Chem. 4 (2013) 5679–5687.
[183] L Chen, Q Yu, Y Wang, H Li, BisGMA/TEGDMA dental composite containing high aspect-ratio hydroxyapatite nanofibers, Dent. Mater. 27 (2011) 1187–1195.
[184] F Gonçalves, C L Azevedo, J L Ferracane, R R Braga, BisGMA/TEGDMA ratio and filler content effects on shrinkage stress, Dent. Mater. 27 (2011) 520–526.
[185] A Amirouche-Korichi, M Mouzali, D C Watts, Shrinkage strain – Rates study of dental composites based on (BisGMA/TEGDMA) monomers, Arab. J. Chem. 10 (2017) S190–S195.
[186] L. Mello de Paiva Campos, L. Cidreira Boaro, H. Perez Ferreira, L.K. Gomes dos Santos, T. Ribeiro dos Santos, D. Fernandes Parra, Evaluation of polymerization shrinkage in dental restorative experimental composites based: BisGMA/TEGDMA, filled with MMT, J. Appl. Polym. Sci. 133 (2016) 43543.
[187] V E S Gajewski, C S Pfeifer, N R G Fróes-Salgado, L C C Boaro, R R Braga, Monomers used in resin composites: degree of conversion, mechanical properties and water sorption/solubility, Braz. Dent. J. 23 (2012) 508–514.
[188] M Bouzrati-Zerelli, M Frigoli, F Dumur, B Graff, J-P Fouassier, J Lalevée, Design of novel photobase generators upon violet LEDs and use in photopolymerization reactions, Polymer 124 (2017) 151–156.
[189] K Arimitsu, R Endo, Application to photoreactive materials of photochemical generation of superbases with high efficiency based on photodecarboxylation reactions, Chem. Mater. 25 (2013) 4461–4463.
[190] S Chatani, T Gong, B A Earle, M Podgorski, C N Bowman, Visible-light initiated thiol-Michael addition photopolymerization reactions, ACS Macro Lett. 3 (2014) 315–318.
[191] B Cohen, D Huppert, Saturation effect in the temperature dependence of a proton recombination with a photobase, J. Phys. Chem. A 106 (2002) 1946–1955.
[192] K Akulov, R Simkovitch, Y Erez, R Gespshtein, T Schwartz, D Huppert, Acid effect on photobase properties of curcumin, J. Phys. Chem. A 118 (2014) 2470–2479.
[193] Y Xie, H L Luk, X Yang, K Glusac, Excited-state hydroxide ion transfer from a model xanthenol photobase, J. Phys. Chem. B 119 (2015) 2498–2506.
[194] X Sun, J P Gao, Z Y Wang, Bicyclic guanidinium tetraphenylborate: a photobase generator and a photocatalyst for living anionic ring-opening polymerization and cross-linking of polymeric materials containing ester and hydroxy groups, J. Am. Chem. Soc. 130 (2008) 8130–8131.
[195] K Arimitsu, R Endo, Photochemical generation of superbases and its application to photoreactive materials, J. Photopol. Sci. Tech. 23 (2010) 135–136.
[196] K Dietliker, R Hüsler, J L Birbaum, S Ilg, S Villeneuve, K Studer, T Jung, J Benkhoff, H Kura, A Matsumoto, H Oka, Advancements in photoinitiators—Opening up new applications for radiation curing, Prog. Org. Coating. 58 (2007) 146–157.
[197] K Dietliker, A Braig, A Ricci, Industrial applications of photochemistry: automotive coatings and beyond, Photochemistry 38 (2010) 344–368.
[198] X Dong, P Hu, G Zhu, Z Li, R Liu, X Liu, Thioxanthone acetic acid ammonium salts: highly efficient photobase generators based on photodecarboxylation, RSC Adv. 5 (2015) 53342–53348.
[199] H Chen, J Yang, D Guo, L Wang, J Nie, Photopolymerization kinetics of α-disulfone cationic photoinitiator, J. Photochem. Photobiol. A Chem. 232 (2012) 57–63.
[200] G Yilmaz, B Iskin, F Yilmaz, Y Yagci, Visible light-induced cationic polymerization using fullerenes, ACS Macro Lett. 10 (2012) 1212–1215.
[201] H Salmi, X Allonas, C Ley, A Defoin, A Ak, Quaternary ammonium salts of phenylglyoxylic acid as photobase generators for thiol-promoted epoxide photopolymerization, Polym. Chem. 5 (2014) 6577–6583.
[202] N Zivic, P K Kuroishi, F Dumur, D Gigmes, A P Dove, H Sardon, Recent advances and challenges in the design of organic photoacid and photobase generators for polymerizations, Angew. Chem. Int. Ed. 58 (2019) 10410–10422.
[203] S Chatani, T Gong, B A Earle, M Podgorski, C N Bowman, ACS Macro Lett. 3 (2014) 315–318.
[204] Dagny D Konieczna, Harry Biller, Matthias Witte, Wolf Gero Schmidt, Adam Neuba, René Wilhelm, New pyridinium based ionic dyes for the hydrogen evolution reaction, Tetrahedron 74 (1) (2018) 142–149, doi:10.1016/j.tet.2017.11.053.
[205] P Xie, F Guo, D Zhang, L Zhang, Dual spectroscopic responses of pyridinium hemicyanine dyes to anions, Chin. J. Chem. 29 (2011) 1975–1981.
[206] Y Ooyama, Y Oda, T Mizumo, J Ohshita, Specific solvatochromism of D-π-A type pyridinium dyes bearing various counter anions in halogenated solvents, Tetrahedron 69 (2013) 1755–1760.
[207] A Reddy Marri, F A Black, J Mallows, E A Gibson, J Fielden, Pyridinium p-DSSC dyes: An old acceptor learns new tricks, Dyes Pigm. 165 (2019) 508–517.
[208] M.-A. Tehfe, A. Zein-Fakih, J. Lalevée, F. Dumur, D. Gigmes, B. Graff, F. Morlet-Savary, T. Hamieh, J.-P. Fouassier, New pyridinium salts as versatile compounds for dye sensitized photopolymerization, Eur. Polym. J. 49 (2013) 567-574.

[209] B Ruiz, M Jazbinsek, P Gunter, Crystal growth of DAST, Cryst. Growth Des. 8 (2008) 4173–4184.
[210] S R Marder, J W Perry, W P Schaefer, Synthesis of organic salts with large second-order optical nonlinearities, Science 245 (1989) 626–628.
[211] A. Schneider, M. Neis, M. Stillhart, B. Ruiz, R. U. A. Khanand P. Gunter, Generation of terahertz pulses through optical rectification in organic DAST crystals: theory and experiment, J. Opt. Soc. Am. 23 (2006) 1822-1835.
[212] H Adachi, K Nagaoka, F Tsunesada, M Yoshimura, Y Mori, T Sasaki, A Sasaki, T Nagatusma, Y Ohiai, N Fukasaku, High-quality crystal growth of organic nonlinear optical crystal DAST, Cryst. Growth Des. 237–239 (2002) 2104–2106.
[213] H. Adachi, Y. Takahashi, J. Yabuzaki, Y. Mori, T. J. Sasaki, Solvent effects and polymorphic transformation of organic nonlinear optical crystal L-pyroglutamic acid in solution growth processes: I. Solvent effects and growth morphology Cryst. Growth Des. 198-199 (1999) 578-582.
[214] M Jazbinsek, L Mutter, P Gunter, Photonic applications with the organic nonlinear optical crystal DAST, IEEE J. Sel. Top. Quantum Electron. 14 (2008) 1298–1311.
[215] T Kaino, B Cai, K Takayama, Fabrication of DAST channel optical waveguides, Adv. Funct. Mater. 12 (2002) 599–603.
[216] J Kabatc, M Zasada, J Paczkowski, Photopolymerization reactions initiated by a visiblelight photoinitiating system: cyanine dye/borate salt/1,3,5-triazine, J. Polym. Sci. A: Polym. Chem. 45 (2007) 3626–3636.
[217] J Kabatc, J Paczkowski, *N*-Methylpicolinium derivatives as the coinitiators in photoinitiating systems for vinyl monomers polymerization, J. Polym. Sci. A: Polym. Chem. 47 (2009) 576–588.
[218] J Kabatc, K Jurek, Free radical formation in three-component photoinitiating systems, Polymer 53 (2012) 1973–1980.
[219] J Kabatc, K Jurek, New two- and three-cationic polymethine dyes. Synthesis, properties and application, Dyes Pigments 112 (2015) 24–33.
[220] R S Davidson, A A Dias, D R Illsley, Type II polymeric photoinitiators (polyetherimides) with built-in amine synergist, J. Photochem. Photobiol. A: Chem. 91 (1995) 153–163.
[221] J Steindl, T Koch, N Moszner, C Gorsche, Silane–acrylate chemistry for regulating network formation in radical photopolymerization, Macromolecules 50 (2017) 7448–7457.
[222] J Kabatc, K Kostrzewska, K Jurek, Two-cationic 2-methylbenzothiazole derivatives as green light absorbed sensitizers in initiation of free radical polymerization, Colloid Polym. Sci. 293 (2015) 1865–1876.
[223] J Kabatc, J Paczkowski, One photon-two free radical photoinitiating systems. Novel approach to the preparation of dissociative, multicomponent, electron-transfer photoinitiators for free radical polymerization, Macromolecules 38 (2005) 9985–9992.
[224] J Kabatc, High speed three-component photoinitiating systems composed of cyanine dyes borate salt and heteroaromatic thiols, Polymer 51 (2010) 5028–5036.
[225] J Kabatc, The cyanine dye/trichloromethyl-1,3,5-triazine/thiols in two- and three-component photoinitiating systems for free radical polymerization, J. Polym. Sci. A Polym. Chem. 48 (2010) 4243–4251.
[226] S Popova, K Pudzs, J Latvels, A Vembris, Light emitting and electrical properties of pure amorphous thin films of organic compounds containing 2-*tert*-butyl-6-methyl-4*H*-pyran-4-ylidene, Opt. Mater. 36 (2013) 529–534.
[227] Y-S Yao, Q-X Zhou, X-S Wang, Y Wang, B-W Zhang, Fine tuning of the photophysical and electroluminescent properties of DCM-type dyes by changing the structure of the electron-donating group, J. Mater. Chem. 16 (2006) 3512–3520.
[228] W Zhou, M-C Wang, X Zhao, Poly(methyl methacrylate) (PMMA) doped with DCJTB for luminescent solar concentrator applications, Sol. Energy 115 (2015) 569–576.
[229] C-B Moon, W Song, M Meng, N H Kim, J-A Yoon, W Y Kim, R Wood, P Mascher, Luminescence of Rubrene and DCJTB molecules in organic light-emitting devices, J. Lumin. 146 (2014) 314–320.
[230] D Xu, Z Deng, X Li, Z Chen, Z Lv, Non-doped red to yellow organic light-emitting diodes with an ultrathin 4-(dicyanomethylene)-2-*tert*-butyl-6-(1,1,7,7-tetramethyljulolidin -4-yl-vinyl)-4*H*-pyran (DCJTB) layer, Phys. E 40 (2008) 2999–3003.
[231] M Kurban, B Gündüz, Physical and optical properties of DCJTB dye for OLED display applications: experimental and theoretical investigation, J. Mol. Struct. 1137 (2017) 403–411.
[232] P Xiao, M Frigoli, F Dumur, B Graff, D Gigmes, J-P Fouassier, J Lalevée, Julolidine or fluorenone based push–pull dyes for polymerization upon soft polychromatic visible light or green light, Macromolecules 47 (2014) 106–112.
[233] T Marinado, D P Hagberg, M Hedlund, T Edvinsson, E M J Johansson, G Boschloo, H Rensmo, T Brinck, L Sun, A Hagfeldt, Rhodanine dyes for dye-sensitized solar cells: spectroscopy, energy levels and photovoltaic performance, PCCP 11 (2009) 133–141.
[234] R Li, L Xie, H Feng, B Liu, Molecular engineering of rhodanine dyes for highly efficient D-π-A organic sensitizer, Dyes Pigm. 156 (2018) 53–60.
[235] B Liu, W Li, B Wang, X Li, Q Liu, Y Naruta, W Zhu, Influence of different anchoring groups in indoline dyes for dye-sensitized solar cells: electron injection, impedance and charge recombination, J. Power Sources 234 (2013) 139–146.
[236] Z Wan, C Jia, Y Wang, X Yao, A strategy to boost the efficiency of rhodanine electron acceptor for organic dye: from non-conjugation to conjugation, ACS Appl. Mater. Interf. 9 (2017) 25225–25231.
[237] B Liu, Q Liu, D You, X Li, Y Naruta, W Zhu, Molecular engineering of indoline based organic sensitizers for highly efficient dye-sensitized solar cells, J. Mater. Chem. 26 (2012) 13348–13356.
[238] P Garra, C Dietlin, F Morlet-Savary, F Dumur, D Gigmes, J-P Fouassier, J Lalevée, Photopolymerization of thick films and in shadow areas: a review for the access to composites, Polym. Chem. 8 (2017) 7088–7101.
[239] P Garra, F Dumur, D Gigmes, A Al Mousawi, H Mokbel, F Morlet-Savary, C Dietlin, J-P Fouassier, J Lalevée, Copper (photo)redox catalyst for radical photopolymerization in shadowed areas and access to thick and filled samples, Macromolecules 50 (2017) 3761–3771.
[240] P K Kaur, R Badru, P P Singh, S Kaushal, Photodegradation of organic pollutants using heterojunctions: a review, J. Env. Chem. Eng. 8 (2020) 103666.
[241] A A Yaqoob, T Parveen, K Umar, M N M Ibrahim, Role of nanomaterials in the treatment of wastewater: a review, Water 12 (2020) 495.
[242] E Talat Helmy, A El Nemr, M Mousa, E Arafa, S Eldafrawy, Photocatalytic degradation of organic dyes pollutants in the industrial textile wastewater by using synthesized TiO_2, C-doped TiO_2, S-doped TiO_2 and C, S co-doped TiO_2 nanoparticles, J. Water Environ. Nanotechnol. 3 (2018) 116–127.
[243] C Santhosh, A Malathi, E Daneshvar, P Kollu, A Bhatnagar, Photocatalytic degradation of toxic aquatic pollutants by novel magnetic 3D-TiO_2@HPGA nanocomposite, Sci. Rep. 8 (2018) 15531.
[244] E Marquez Brazon, C Piccirillo, I S Moreira, P M L Castro, Photodegradation of pharmaceutical persistent pollutants using hydroxyapatite-based materials, J. Environ. Manage. 182 (2016) 486–495.
[245] W Deng, H Zhao, F Pan, X Feng, B Jung, A Abdel-Wahab, B Batchelor, Y Li, Visible-light-driven photocatalytic degradation of organic waterpollutants promoted by sulfite addition, Environ. Sci. Technol. 51 (2017) 13372–13379.
[246] M Ghali, C Brahmi, M Benltifa, F Dumur, S Duval, C Simonnet-Jégat, F Morlet-Savary, S Jellali, L Bousselmi, J Lalevée, Synthesis of polyoxometalate/polymer composites under soft conditions for enhancement of dye photodegradation by photocatalysis, J. Polym. Sci. A Polym. Chem. 57 (2019) 1538–1549.